The 700-1500 cm1 region of the S1 (A 1 B 2) state of toluene studied with resonance-enhanced multiphoton ionization (REMPI), zero-kinetic-energy (ZEKE) spectroscopy, and time-resolved slow-electron velocity-map imaging (tr-SEVI) spectroscopy

Adrian M. Gardner, Alistair M. Green, Victor M. Tamé-Reyes, Katharine L. Reid, Julia A. Davies, Victoria H. K. Parkes, and Timothy G. Wright

Citation: The Journal of Chemical Physics **140**, 114308 (2014); doi: 10.1063/1.4867970
View online: http://dx.doi.org/10.1063/1.4867970
View Table of Contents: http://scitation.aip.org/content/aip/journal/jcp/140/11?ver=pdfcov
Published by the AIP Publishing

The 700-1500 cm^{-1} region of the S_1 ($\tilde{A}^1B_2$) state of toluene studied with resonance-enhanced multiphoton ionization (REMPI), zero-kinetic-energy (ZEKE) spectroscopy, and time-resolved slow-electron velocity-map imaging (tr-SEVI) spectroscopy

Adrian M. Gardner,[a] Alistair M. Green, Victor M. Tamé-Reyes, Katharine L. Reid, Julia A. Davies,[b] Victoria H. K. Parkes,[c] and Timothy G. Wright[d]
School of Chemistry, University of Nottingham, University Park, Nottingham NG7 2RD, United Kingdom

(Received 20 December 2013; accepted 25 February 2014; published online 19 March 2014)

We report (nanosecond) resonance-enhanced multiphoton ionization (REMPI), (nanosecond) zero-kinetic-energy (ZEKE) and (picosecond) time-resolved slow-electron velocity map imaging (tr-SEVI) spectra of fully hydrogenated toluene (Tol-h_8) and the deuterated-methyl group isotopologue (α_3-Tol-d_3). Vibrational assignments are made making use of the activity observed in the ZEKE and tr-SEVI spectra, together with the results from quantum chemical and previous experimental results. Here, we examine the 700–1500 cm^{-1} region of the REMPI spectrum, extending our previous work on the region $\leq$700 cm^{-1}. We provide assignments for the majority of the S_1 and cation bands observed, and in particular we gain insight regarding a number of regions where vibrations are coupled via Fermi resonance. We also gain insight into intramolecular vibrational redistribution in this molecule. © *2014 AIP Publishing LLC*. [http://dx.doi.org/10.1063/1.4867970]

I. INTRODUCTION

A. Background to the spectroscopy

Toluene (methylbenzene) is the simplest substituted benzene to contain a methyl group. Formally, it possesses 39 normal vibrational modes, although one of these may be more properly considered as an internal rotation, or "torsion," of the methyl group. In a previous paper,[1] we have discussed the vibrational wavenumbers of the ground electronic state, for which values for most modes have been established, but several are still uncertain. The assignment employed a vibrational mode labeling scheme for the non-substituent-localized vibrations of the monosubstituted benzenes.[2] This scheme treats the substituent as a point mass and allows the identification of the ring-localized vibrations by a label, M_i, where the label indicates the vibration of fluorobenzene which most closely resembles the monosubstituted benzene vibration: this can be done "by eye," or via a Duschinsky matrix approach—the reader is referred to Ref. 1 and particularly to Ref. 2 for further details. (Note that in Refs. 1 and 2, we used a script M to label the vibrational labels, but it has proven difficult to maintain consistency between journal text and figures, so we shall switch to the more straightforward italicized M here and in future publications.) For clarity, in Table I we present the correspondence between the common labeling schemes used for toluene; we note that the actual forms of the vibrations are presented in Figure 5 of Ref. 2. We note that Hickman *et al.*[3] based their numbering on the Herzberg[4] (or Mulliken[5]) scheme, assuming a C_{2v} molecule (i.e., assuming the methyl group is a point mass). The numbering is not clear however, as the methyl vibrations have been included in the list, and these cannot be described in terms of C_{2v} labels. (In fact, the C_s group should more properly be used, but then all of these labels would change.) Varsányi[6] based his labels on those of Wilson,[7] but used different labels for the same vibrational motion, depending on whether a substituent was "heavy" or "light." Additionally, the actual motion was often very different from the benzene mode with the same label—this is indicated by the very mixed character of these modes (see Ref. 2). These points have been discussed in detail in Ref. 2 and are not rehearsed further in the present work.

Assuming C_{2v} symmetry, the electronic transition $S_1 \leftarrow S_0$ corresponds to the promotion of an electron from the highest occupied molecular orbital with b_1 symmetry, to the lowest unoccupied orbital of a_2 symmetry, and so the transition can also be written $\ldots(b_1)^1(a_2)^1\tilde{A}^1B_2 \leftarrow \cdots(b_1)^2(a_2)^0\tilde{X}^1A_1$. Hickman *et al.*[3] have recorded a fluorescence excitation spectrum for toluene in a jet-cooled molecular beam, extending to ~2000 cm^{-1} internal energy for the S_1 state. The majority of the observed absorption features were identified with the aid of dispersed fluorescence, making use of the known S_0 frequencies to support these assignments. These measurements yielded frequencies for 13 normal modes in the S_1 excited state. When exciting via higher-wavenumber features, rather than the well-structured spectra recorded *via* lower wavenumber levels, several of the spectra showed considerable loss of structure, which was concluded to be a result of intramolecular vibrational redistribution (IVR)—see Subsection I B.

[a]Present address: Department of Chemistry, Chemistry Building, Emory University, Atlanta, Georgia 30322, USA.
[b]Present address: Department of Chemistry, Imperial College London, Exhibition Road, London SW7 2AZ, United Kingdom.
[c]née Wilton.
[d]Author to whom correspondence should be addressed. Electronic mail: Tim.Wright@nottingham.ac.uk

TABLE I. Correspondence between the M_i labeling scheme and those used by previous workers.

M_i[a]	Ref. 3	Varsányi[6,b]
	a_1	
1	1	20a
2	2	2
3	3	7a
4	5	9a
5	6	18a
6	8	13
7	9	8a
8	10	19a
9	11	12
10	12	1
11	13	6a
	a_2	
12	14	17a
13	15	10a
14	16	16a
	b_1	
15	20	5
16	21	17b
17	22	11
18	23	4
19	24	16b
20	25	10b
	b_2	
21	26	7b
22	27	20b
23	29	9b
24	31	18b
25	32	3
26	33	8b
27	34	14
28	35	19b
29	37	6b
30	38	15
	Methyl-localized	
...	17	ν_{as}
...	28	ν_{as}
...	4	ν_s
...	30	δ_{as}^+
...	18	δ_{as}^+
...	7	δ_s
...	19	δ_{as}^-
...	36	δ_{as}^-

[a]The actual forms of the vibrations are presented in Figure 5 of Ref. 2.

[b]The motions of the Varsányi modes are not the same as the Wilson modes, nor are they the same as the M_i motions (see Fig. 5 of Ref. 2); the latter give a more realistic picture of the actual vibrational modes, and hence which atoms are moving, and so how one expects vibrations to shift upon deuteration.

In an early study, Meek *et al.*[8] recorded a one-colour, two-photon multiphoton ionization photoelectron spectrum, MPI-PES, of Tol-h_8 seeded in an effusive molecular beam using an intermediate level lying 932 cm^{-1} above the S_1 origin, labelled as mode 12 in the Wilson notation used therein (assigned to M_8 in the below). The two-photon photoelectron spectrum was considerably congested, as a consequence of simultaneous excitation of sequence bands, along with the targeted S_1 vibration. Whiteside *et al.*[9] have used both nanosecond and picosecond lasers to record photoelectron spectra *via* several intermediate vibrations in this wavenumber range of the S_1 electronic state of Tol-h_8. In the nanosecond experiments, the photoelectron spectra were very congested, showing very little structure. Using two spatially and temporally overlapped picosecond pulses to excite and ionize toluene seeded in a molecular beam, some structure was retained in the photoelectron spectra; however, considerable congestion was still observed, concluded to be a result of very fast IVR processes occurring at the wavenumbers employed.

In the present work, one-colour (1 + 1) resonance-enhanced multiphoton ionization (REMPI) spectra between 700 and 1500 cm^{-1} for both the fully hydrogenated toluene (Tol-h_8) and the deuterated-methyl group isotopologue (Tol-d_3) are presented, and the assignment discussed. As in our previous paper,[1] two-colour zero-kinetic-energy (ZEKE) spectra were also recorded *via* several of the observed levels in order both to aid assignment of the S_1 vibrations, and to investigate the previously reported loss of structure observed, particularly in the photoelectron spectra recorded *via* these levels. In a recent publication,[10] we reported the results of picosecond time-resolved slow electron velocity map imaging (tr-SEVI), investigating a Fermi resonance at ~1190 cm^{-1}. The latter paper will be discussed further below when considering the results of the present paper; additionally, further tr-SEVI results are presented for other features observed in the $S_1 \leftarrow S_0$ REMPI spectra.

B. Background to intramolecular vibrational redistribution

In this section, we outline the process of intramolecular IVR in toluene, first clarifying the nomenclature used and the nature of the coherent excitation process in the tr-SEVI experiments. We shall also provide some remarks on the different IVR regimes. As will be seen below, and also in recent previous work[1,10,18] there are regions of the toluene REMPI spectrum that have a number of vibrational features close together in wavenumber. As such, it is possible that these arise as a result of Fermi resonance (FR), whereby two so-called zero-order states (ZOSs) interact and form two new vibrational eigenstates. Potentially, FR can occur between any two states of the correct symmetry, which are close together; however, it is particularly interesting when one of the states is optically dark, while the other is optically bright (indeed, this is the strict definition of a Fermi resonance). In this case, the states interact and yield two vibrational eigenstates which both have bright character, and so an "extra" band appears in the spectrum; additionally, the vibrational eigenstates will be shifted from the expected ZOS positions. The two ZOSs can be termed the zero-order bright state (ZOB) and the zero-order dark state (ZOD). If the two eigenstates are sufficiently close in wavenumber that they can be excited coherently, then a wavepacket is formed that is a superposition of the two vibrational eigenstates. Under these circumstances, time-dependent behavior can be observed as the resulting wavepacket evolves. At $t = 0$, this wavepacket will look like the ZOB, while later on it will look like the

ZOD and if no other processes occur, then this oscillation in wavepacket character will continue with an angular frequency of $2\pi\nu$ rad s^{-1}, where $\nu = \Delta E/h$ and ΔE is the energy difference between the two eigenstates. It is this temporal change in vibrational character that leads to the term IVR, as it may be viewed as energy moving between different ZOSs; although it is important to stress that the population of the vibrational eigenstates does not change during the IVR process (assuming no additional photophysical processes occur).

Of course, if more than two ZOSs are in close proximity and are of the correct symmetry, then these can all interact—this may be termed a complex Fermi resonance. In this case, it may be that two or more of the ZOSs are bright/dark and various "extra" bands may appear in the spectrum and, of course, be shifted from the expected ZOS positions.

In our nanosecond ZEKE experiments, we are always exciting with a narrow bandwidth and so can generally pick out the individual vibrational eigenstates. If the corresponding cation vibrational states are well separated in energy (i.e., the corresponding ZOSs in the cation are not interacting), then the ZEKE spectrum will show clearly separated features originating from both the S_1 bright and dark states, since both are contributing to the vibrational eigenstate excited. In this way, the assignment of the ZEKE spectrum allows insight into the make-up of the vibrational eigenstates.

In our picosecond experiments, a coherent vibrational wavepacket is created if the Fermi resonance components lie within the laser bandwidth (FWHM ~13 cm^{-1}). Ionization using a second picosecond pulse at a series of delays allows time-dependent behavior to be observed by recording photoelectron spectra, which are "snapshots" of the wavepacket at the instant of ionization. Monitoring changes in the photoelectron spectrum with time can then give insight into the S_1 vibrational eigenstate make-up, provided the spectrometer's resolution is sufficient to observe individual vibrationally resolved photoelectron bands, and provided these can be assigned. In the present work, the required resolution is met by recording tr-SEVI – see below for further details. Of course, if the Fermi resonance components do not lie within the bandwidth of the laser, single vibrational eigenstates are excited, as in the nanosecond experiments, and therefore no time dependence is expected in the photoelectron spectrum, ignoring other possible population depletion pathways such as intersystem crossings, internal conversion or fluorescence.

Fermi resonances between a small number of ZOSs are the simplest type of IVR process; however, as the density of vibrational states increases, then it is possible for different tiers of interactions to be identified.[11] Once the density of vibrational states becomes high, then these form a bath of states which can couple the ZOSs via various mechanisms; so any ZOB, for example, can couple to this bath. Some states will be more efficiently coupled to the bath than others, and can then provide a route for other ZOSs to become coupled to the bath: such states have been termed doorway states (see Ref. 11 and references therein).

As will be seen in the below, the ZEKE and tr-SEVI results are complementary in the present work and the combined results give detailed insight into the IVR processes, including the identification of doorway states.

II. EXPERIMENT

The REMPI and ZEKE apparatus employed has been described previously in detail elsewhere,[1,12,13] and so only a brief description is given here. The second (532 nm) and third (355 nm) harmonics of a neodymium-doped yttrium aluminium garnet laser (Nd:YAG, Surelite III, 10 Hz) were each used to pump one of two tunable dye lasers (Sirah Cobra Stretch). The pump dye laser was operated on Coumarin 503 (355 nm pump), while Pyrromethene 597 (532 nm pump) was used in the ionization laser. The fundamental output of each dye laser was frequency doubled using β-barium borate (BBO) and potassium dihydrogen phosphate (KDP) crystals for the pump and probe lasers, respectively.

Tol-h_8 (Acros, 99.5% purity) or Tol-d_3 (Aldrich, 99 atom% D) vapour was seeded in ~2 bars of Ar and the gaseous mixture passed through a General Valve pulsed nozzle (750 μm, 10 Hz, opening time of 210 μs) to create a free jet expansion. The focused, frequency-doubled output of both dye lasers were overlapped spatially and temporally and passed through a vacuum chamber coaxially and counterpropagating. Here, they intersected the free jet expansion between two biased electrical grids located in the extraction region of a time-of-flight mass spectrometer.

One-colour, (1 + 1) REMPI spectroscopy was utilized in order to determine the pump frequencies required to prepare each vibrational level in the S_1 state of toluene selectively. When moving to the two-colour experiments, the intensities of the two overlapped laser beams were then adjusted by monitoring the large enhancement of the ion signal arising from the (1 + 1′) process. The voltages on the lens assembly were then changed for the pulsed-field ionization, zero-electron-kinetic energy (PFI-ZEKE) photoelectron spectroscopy. The upper lens element was terminated to ground, while a fast rising pulsed positive potential was applied to the lower plate, both to pulse-field ionize high-lying Rydberg states and also to extract the resulting ZEKE electrons. For the present experiments, it was found that a field of 5 V cm^{-1} resulted in the most intense ZEKE signals. The electrons were detected via a second dual microchannel plate detector, which was located ~2 cm below the electrical extraction grids.

As noted in the previous experiments,[1] it was confirmed that, in line with conclusions reached by Bacon and Hollas,[14] the photoionization cross-section for toluene was about an order of magnitude lower than that of the *para*-fluorotoluene (pFT) molecule we have studied previously;[15] as such, there was a continual compromise between resolution and signal-to-noise ratios in the ZEKE spectra and this limited the range of S_1 resonances we could employ as intermediates. In most cases in the present work, we estimate a typical ZEKE resolution of ~8-10 cm^{-1}, and from approximate rotational simulations of the S_1 bands observed we estimate a typical rotational temperature of ~5 K, although under the best conditions, rotational temperatures of ~2 K could be obtained.

The excitation laser has been calibrated with an absolute error of ±1 cm^{-1} by comparison of the bands observed in the (1 + 1) REMPI spectrum in the present work and the fluorescence excitation spectrum reported by Hickman *et al.*,[3] with the origin position calibrated to that reported by Borst

and Pratt.[16] Use was also made of the known positions of the S_1 origin of *p*FT,[15] observed in a recent series of experiments. We estimate our relative error to be approximately ± 0.5 cm^{-1}. Calibration of the ionization laser has been performed through comparison of the ZEKE bands observed in the present and previous work,[1] and those seen for toluene by Lu *et al.*[17] and we estimate an absolute and relative error of ± 1 cm^{-1} in the ZEKE peak positions.

For the tr-SEVI experiments, the picosecond laser system (Coherent), velocity-map imaging (VMI) photoelectron spectrometer, experimental procedures and data analysis techniques used in the picosecond experiments have been described elsewhere[18,19] and are not reproduced in detail here. Briefly, the two UV outputs from the laser system have pulse durations of 1 ps and bandwidths of $\sim$13 cm^{-1}. The co-propagating laser beams were focused into the VMI chamber using a 1.0 m focal length lens, resulting in typical pump and probe pulse intensities of 5×10^9 W/cm^2 and 1×10^{11} W/cm^2, respectively. The wavelength of the pump beam was tuned to be resonant with features of interest in the S_1 spectrum; the probe wavelength was then tuned in steps to access ranges of the cation internal states of interest. The samples of Tol-h_8 and Tol-d_3 were seeded in 3 bars He and expanded through a pulsed nozzle (General Valve) operating at a repetition rate of 40 Hz. The supersonic expansion was skimmed leading to a molecular beam with a rotational temperature of $\sim$10 K. Inside the spectrometer chamber, the laser beams were spatially and temporally overlapped with the pulsed molecular beam; the typical operating pressure was 4×10^{-8} mbar. A delay stage enabled the selection of chosen time intervals between the pump excitation pulse and the probe ionization pulse in order to monitor time-dependent behavior. A three-element electrostatic lens focused the electrons onto a vacuum imaging detector (VID, Photek) to create a two-dimensional image, which was captured using a CCD camera and recorded using IFS32 software (Photek). Using this technique we were able to record photoelectron images as a function of both pump-probe time delay and probe wavelength. These images were converted to give photoelectron spectra as discussed in earlier work.[18] Photoelectron angular distributions were also obtained from the images but they showed no significant changes with time delay and will not be discussed further. The imaging detector can also be operated in ion detection mode to measure mass-resolved REMPI spectra via the S_1 state of each molecule.

III. RESULTS AND ASSIGNMENT

A. General remarks

As we highlighted in Ref. 2, there have been a number of inconsistencies in applying Wilson labels[7] to some of the vibrational modes in benzene, which has been propagated into work on substituted benzenes. We do not reproduce the details here, but note that some or all of the following switches in Wilson mode numbering for benzene are often required in order to assign the correct wavenumber to the correct vibrational motion: 8a $\leftrightarrow$ 9a, 8b $\leftrightarrow$ 9b, 18a $\leftrightarrow$ 19a, 18b $\leftrightarrow$ 19b, and 3 $\leftrightarrow$ 14. Our new nomenclature[2] employs the Mulliken labeling scheme[5] for fluorobenzene, but then maintains the same label across different monosubstituted benzenes, even when the symmetry of the molecule and overall number of vibrations has changed. This leads to a much clearer understanding of the vibrational activity in these species. To aid the reader, in Table I we present the numbering used in Ref. 3, which is not strictly Herzberg (Mulliken) numbering as the methyl-localized vibrations have been mistakenly included in the list, and also the Varsányi labels, whose motion does not always correspond to the actual motion – see Ref. 2 for further discussion.

The (1 + 1) REMPI spectra of Tol-h_8 and Tol-d_3 $< \sim$1460 cm^{-1} above the S_1 origin are shown in Figure 1. The large number of vibrations observed above 700 cm^{-1} is striking. As in the lower wavenumber range, the overall appearance of the Tol-h_8 spectrum is similar to previously reported jet-cooled spectra.[3,20,21] There are several intense bands observed above 700 cm^{-1}, which have mainly been assigned to vibrations of a_1 symmetry; however, several combination bands of overall b_2 symmetry are observed, which owe their intensity to Herzberg-Teller coupling to the S_2 electronic state.

In the following, the assignments of the Tol-h_8 and Tol-d_3 (1 + 1) REMPI spectra in the range 700–1500 cm^{-1} will be discussed simultaneously, separating the discussion into different wavenumber ranges. The assignment will employ the results of quantum chemical calculations, plus the concomitant discussion of the ZEKE spectra recorded in the present work, exciting through features in the above wavenumber range. The identification of overtones and combination bands will benefit from the assignments of features $<$700 cm^{-1} performed in our previous work.[1] In Ref. 1, we presented harmonic and anharmonic values for the S_0 and D_0^+ states, plus the harmonic values for the S_1 states; all calculated using the B3LYP functional and the aug-cc-pVTZ basis set, with time-dependent density functional theory (TD-DFT) employed for the S_1 state. In the present work, in Table II, we present the anharmonic results for the S_0 and D_0^+ states, together with scaled harmonic results ($\times$0.97) for all three states. In fact, we find that often the scaled harmonic values are more reliable than the anharmonic ones. Additionally, where available, we also give the experimentally determined values.

In the below, we present the assignments of the spectra, separated into convenient wavenumber ranges. We base the assignments on different pieces of experimental evidence: the experimentally derived values from our previous work,[1] the assignments made in the dispersed fluorescence study of Ref. 3, and the calculated vibrational frequencies in Table II. We obviously favour the experimentally derived values where they exist, but in many cases we have to rely on the calculated values. For the S_0 and D_0^+ states, the agreement between the anharmonic and scaled vibrational wavenumbers is generally very good; in the cases where the agreement is not so good, we consider both values, and exercise caution, but generally favour the scaled value. (We assume that in some cases the anharmonic values, obtained from perturbation methods, are affected by close degeneracies.)

We now consider the assignment of the REMPI spectra, separating the discussion into different spectral ranges. In

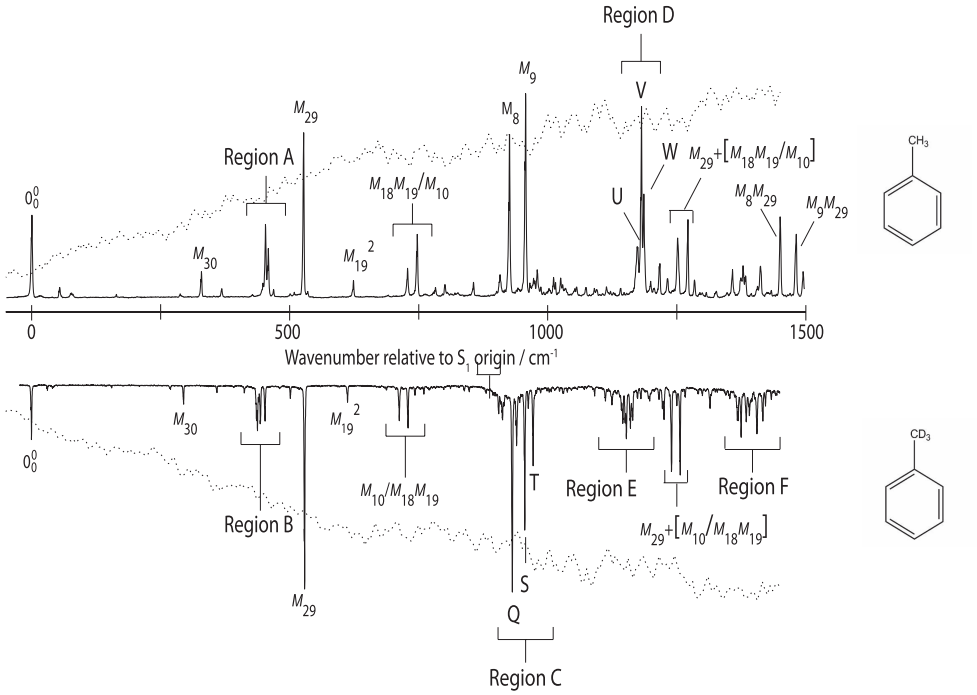

FIG. 1. (1 + 1) REMPI spectra of Tol-h_8 (upright) and Tol-d_3 (inverted) in the range 0–1500 cm^{-1} for Tol-h_8 and 0–1450 cm^{-1} for Tol-d_3. The dotted lines indicate the intensity of the UV radiation across the region.

each of these ranges, we shall consider both Tol-h_8 and Tol-d_3 REMPI spectra, and the resulting ZEKE spectra.

B. 680–880 cm^{-1} region

The expanded REMPI spectra in this wavenumber region for both Tol-h_8 and Tol-d_3, are shown in Figure 2(a). Two features are observed at 734.4 and 753.2 cm^{-1} for Tol-h_8, which are labeled "M" and "N"; these have been previously assigned as a Fermi resonance between two ZOS vibrations.[21,22] The assignment of the higher wavenumber vibrational eigenstate has been long-established as having a major contribution from the M_{10} fundamental,[3,21,22] while Hickman *et al.*[3] assigned the other ZOS of the Fermi resonance to the $M_{18}M_{19}$ combination. This assignment was based on the vibrational activity in the dispersed fluorescence spectrum recorded from these intermediate levels, and is expected to form the major contribution to the lower wavenumber component of the Fermi resonance. This situation is largely reminiscent of the major aspect of the Fermi resonance observed at ∼460 cm^{-1} in the S_1 electronic state of Tol-h_8: a combination of two out-of-plane vibrations interacting with an a_1 fundamental vibration. The 460 cm^{-1} feature has been discussed in depth by ourselves[1,18] and by Gascooke and Lawrance[23] in their two-dimensional laser-induced fluorescence (2D-LIF) study concentrating on the same feature. Owing to the expected significant contributions of each of the two ZOSs to the vibrational eigenstates giving rise to M and N, the bands are not given explicit mode labels in Figure 2(a).

By visual inspection of the REMPI spectra in Fig. 2(a), bands O and P in the Tol-d_3 REMPI spectrum can be expected to be made up of the same ZOSs as those that contribute to the vibrational eigenstates that give rise to bands M and N for Tol-h_8, although we would expect the ZOS weightings to be different.

ZEKE spectra have been recorded *via* bands M and N for Tol-h_8 and *via* bands O and P for Tol-d_3, and these are shown in Figures 2(b) and 2(c), respectively. These spectra are somewhat noisy, with the vibrational features appearing to be superimposed on an underlying background; the origin of the latter observation will be discussed below.

The ZEKE spectrum recorded *via* band M, shows two clear bands, with the lower wavenumber, weaker band at 768 cm^{-1} being assignable to M_{10}^+, based on the assignment of this fundamental wavenumber in Ref. 1 and the calculated vibrational wavenumbers in Table II; the more intense band at 941 cm^{-1} is assignable to $(M_{18}M_{19})^+$; both combination bands with the M_{11}^+ vibration are also observed weakly. The ZEKE spectrum recorded *via* N shows the same two features, now having similar intensities to each other. The assignments of the cationic vibrations are consistent with the S_1 assignments of Hickman *et al.*[3] based on their DF spectra, to a pair of Fermi resonance components involving the M_{10} and $M_{18}M_{19}$ vibrations. Using the experimentally derived fundamental wavenumber of the M_{18}^+ vibration of Tol-h_8, 566 cm^{-1} and the 377 cm^{-1} value for the M_{19}^+ fundamental, then a combination wavenumber of 943 cm^{-1} is obtained, in excellent agreement with the experimental value.

The earlier reported photoelectron spectrum of Tol-h_8, recorded using laser pulses of ∼5 ns by Whiteside *et al.*[9] and exciting *via* band N (based on the cited wavenumber) contains limited structure and is very congested; this is in contrast to the present spectra and the DF spectra of Ref. 3.

The assignment of the two ZOSs that give rise to the bands observed in the REMPI spectrum at 712.6 and 729.6 cm^{-1} of Tol-d_3, are expected to be the same as those

TABLE II. Calculated vibrational wavenumbers of Tol-h_8 and Tol-d_3. These are calculated using the B3LYP/aug-cc-pVTZ level of theory, with the scaled values being 0.97× harmonic. (The unscaled harmonic and anharmonic values are presented in Ref. 1, together with the values for the methyl-localized vibrations.)

	Tol-h_8					Tol-d_3				
	S_0		S_1	D_0		S_0		S_1	D_0	
Mode, M_i	Scaled	Anharmonic	Scaled	Scaled	Anharmonic	Scaled	Anharmonic	Scaled	Scaled	Anharmonic
					a_1					
1	3093	3045	3117	3117	3076	3093	3045	3117	3117	3076
2	3073	3036	3095	3103	3069	3073	3037	3095	3103	3077
3	3059	2999	3088	3094	3069	3059	2990	3087	3094	3060
4	1596	1604	1531	1622	1576	1596	1606	1531	1622	1568
5	1486	1499	1414	1430	1431	1486	1500	1415	1432	1444
6	1193	1202	1184	1220	1227	1212	1218	1210	1240	1253
7	1168	1191	1142	1181	1186	1168	1195	1143	1185	1189
8	1021	1035	945	958	984	1018	1033	944	952	967
9	991	1008	960	979	982	991	1008	962	974	983
10	776	786	745	753	762	750	761	718	727	740
11	513	525	452	504	508	491	501	436	476	476
					a_2					
12	964	976	697	996	1010	965	982	697	993	1006
13	837	848	562	784	774	836	848	562	783	770
14	404	409	210	340	348	404	411	210	340	351
					b_1					
15	983	995	797	1008	1049	984	996	806	1008	1044
16	893	902	695	919	930	839	842	675	952	969
17	728	740	581	731	736	704	710	576	681	683
18	695	705	437	564	583	683	694	417	520	541
19	464	474	312	374	388	446	452	308	366	379
20	204	210	146	147	154	189	197	138	139	146
					b_2					
21	3081	3033	3108	3114	3046	3081	3017	3108	3114	3100
22	3060	3016	3089	3098	3065	3060	3021	3089	3098	3065
23	1575	1584	1493	1364	1380	1571	1584	1488	1364	1373
24	1428	1441	1426	1492	1499	1438	1454	1378	1492	1499
25	1321	1343	1373	1352	1352	1319	1331	1287	1350	1355
26	1287	1286	1140	1258	1264	1281	1307	1140	1259	1265
27	1146	1168	1398	1128	1147	1146	1169	1407	1120	1133
28	1079	1092	1027	1052	1069	1071	1084	995	1052	1072
29	619	633	522	485	493	618	631	520	492	500
30	333	364	329	336	330	297	310	293	299	297

of Tol-h_8; i.e., these are two components of a Fermi resonance with the same ZOSs. The M_{10}^+ fundamental wavenumber of Tol-d_3 has been determined as 742 cm^{-1} from the ZEKE spectrum recorded *via* the S_1 0^0 level, discussed in Ref. 1, which is in very good agreement with the peak position of 741 cm^{-1} for the more intense feature in the ZEKE spectrum recorded *via* band O; this is also supported by the calculated vibrational frequencies in Table II. The more intense ZEKE band is at 893 cm^{-1} and is assignable to the $(M_{18}M_{19})^+$ combination vibration through comparison with the corresponding band observed in the spectrum recorded *via* band M of Tol-h_8. The same two bands are also seen when exciting via band O, but with reversed intensities. Using the experimentally derived fundamental wavenumber of the M_{18}^+ vibration of Tol-d_3, 528 cm^{-1}, a wavenumber of 366 cm^{-1} for the M_{19}^+ fundamental is obtained, in very good agreement with the calculated values, shown in Table II. We shall discuss these Fermi resonances in more detail below.

A further observation may be made regarding the ZEKE spectrum recorded *via* band N, in which a number of features are present which are not observed in the corresponding spectrum recorded *via* band M; itself an interesting observation given that M and N arise from Fermi resonance components. Most of these are straightforwardly assigned, as shown in Figure 2 on the basis of previously observed and calculated vibrational wavenumbers; however, the band at 822 cm^{-1}—labeled "x" in the upper trace of Figure 2(c)—is less straightforward. It is interesting to note that an extra band at 922 cm^{-1} was also observed in the DF spectra reported by Hickman *et al.*[3] recorded *via* the band N. Although they were unable to provide an assignment for this band, it was hypothesised that its origin was another vibration, whose feature lay completely within the unresolved rotational contour of band N. If this is

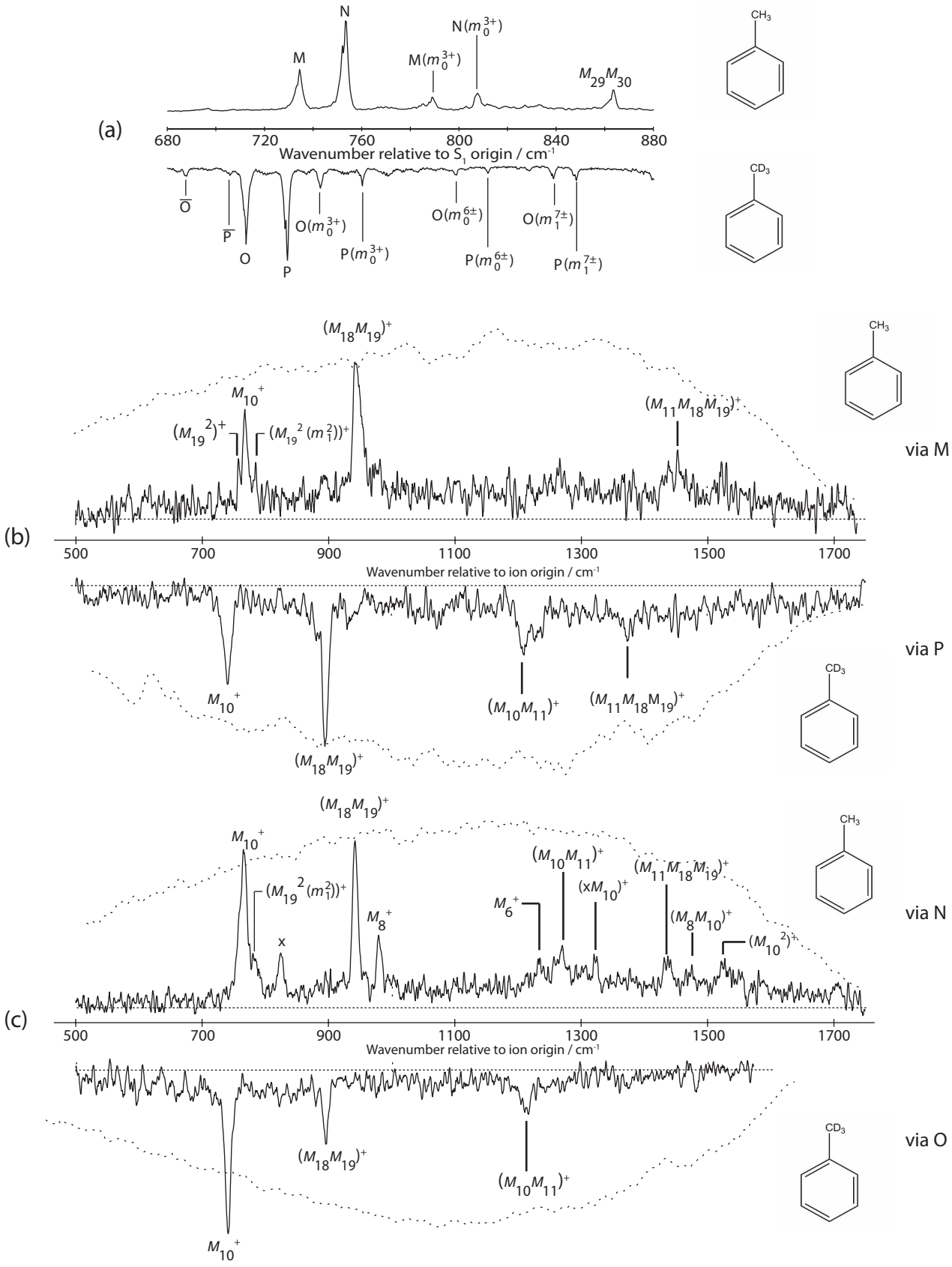

FIG. 2. (a) Expanded view of the Fermi resonance region of the (1 + 1) REMPI spectra of Tol-h_8 (upright) and Tol-d_3 in the range 680–880 cm^{-1}. Traces (b) and (c) contain ZEKE spectra recorded *via* eigenstates designated by the letters in the top trace of the REMPI spectrum. Spectra for Tol-h_8 and Tol-d_3 have been paired up based on their appearance and assignment: see text. The assignment of bands marked with letters are discussed in the text. The dotted lines indicate the intensity of the UV radiation across the region.

the case, then we should see ZEKE features arising from this coincident vibration; the relatively intense feature "x" could be such a feature. We now discuss whether band x could be the analogue of the prominent band observed at 922 cm^{-1} in the DF spectrum recorded *via* band N by Hickman *et al.*[3] If this was the case, then the likely assignment of both features would be a $\Delta v = 0$ transition originating from the hypothesised coincident vibration in the S_1 state and the vibration would be expected to have wavenumbers of ~922, ~754, and ~822 cm^{-1} in the S_0, S_1, and D_0^+ electronic states, respectively.

No assignment was found, in terms of fundamentals, overtones, or combinations, that match the observed wavenumbers in all three states. For example, of the possible vibrational (and vibration-torsion) levels predicted to have S_1 vibrational wavenumbers of 754 ± 10 cm^{-1}, only two result in cationic vibrational wavenumbers within 822 ± 10 cm^{-1}: the $M_{14}^1M_{29}^1$ and $M_{19}^1M_{20}^3$ combinations. However, neither of these possibilities has a corresponding S_0 vibrational wavenumber which matches the unassigned band observed at 922 cm^{-1} in the DF spectrum. Hence, separate vibrational assignments of the observed bands in the S_0 and D_0^+ states were sought. The $(M_{29}M_{30})^+$ combination is a possible assignment of band x and we note this combination is also active in the $S_1 \leftarrow S_0$ transition (see upper trace of Figure 2(a), and below). A possible assignment of the 922 cm^{-1} band in S_0 is to M_{19}^2, based on the fundamental value of 464 cm^{-1} for this mode, reported in Ref. 3. Overall, there does not seem to be strong evidence for a second feature coincident with band N; whether such a feature exists or not, the differing observed activity in the DF and ZEKE spectra suggests different Franck-Condon factors (FCFs) occur during the fluorescence and ionization processes.

The fundamental value of 695 cm^{-1} for the M_{18} mode in S_0 state (see Ref. 1) suggests a value of ~1390 cm^{-1} for M_{18}^2, which matches well with the band observed at 1380 cm^{-1} in the DF spectrum recorded *via* the S_1 753.2 cm^{-1} intermediate;[3] this band was also observed in the DF spectrum recorded *via* the S_1 734.4 cm^{-1} level. Assuming these assignments are correct it is interesting that the M_{19}^2 vibration is only observed in the dispersed fluorescence spectrum recorded *via* the higher wavenumber Fermi resonance component. This is in line with the observations of the ZEKE spectra via bands M and N which also show different vibrational activity.

In Ref. 1, we discussed the similarity of the toluene electronic spectra with those of fluorobenzene and chlorobenzene, the observation of which was impetus for the development of the vibrational notation used herein; as a consequence, we looked for possible assignments from the DF spectra of those species. In fluorobenzene,[24] the eigenstate assigned to contain a larger contribution from the M_{10} zero-order state lies at 765 cm^{-1}, which is below the other Fermi resonance component observed at 781 cm^{-1}, notably the same ordering as observed for Tol-d_3. The DF spectra recorded *via* these intermediate levels show similar, but interesting intensity effects: along with the expected $M_{18}M_{19}$ and M_{10} vibrations being observed, the M_{19}^2 vibration is also clearly seen. Rather surprisingly, the M_{18}^2 vibration is observed only weakly in the DF spectrum recorded *via* the lower wavenumber component of the Fermi resonance, despite being observed strongly in the DF spectrum recorded *via* the other Fermi resonance component. Although the "absent" overtone is different in the DF spectra of Tol-h_8 and fluorobenzene, this observation does suggest that the assignments of the M_{19}^2 and M_{18}^2 vibrations in the toluene DF spectra are likely correct. Unfortunately, the corresponding DF spectra have not been recorded for chlorobenzene which would allow the activity of the M_{18}^2 and M_{19}^2 vibrations to be investigated further.

With the above discussion in mind, we note that the M_{19} and M_{18} fundamental vibrations have been observed in the Tol-h_8 ZEKE spectrum recorded *via* the S_1 origin, discussed in Ref. 1, which have vibrational wavenumbers of 377 cm^{-1} and 566 cm^{-1}, respectively. Utilizing these values, the $(M_{19}^2)^+$ and $(M_{18}^2)^+$ vibrations have expected vibrational wavenumbers of 758 and 1132 cm^{-1}, respectively. The $(M_{19}^2)^+$ value is in remarkably good agreement with the 757 cm^{-1} band observed in the ZEKE spectrum obtained when exciting via band M. Owing to the close proximity of the $(M_{19}^2)^+$ overtone to the M_{10}^+ vibration, they could be in Fermi resonance, the result of which could perturb the Franck-Condon factors for ionization to the M_{10}^+ vibration.

The fundamental wavenumber of 366 cm^{-1} for the M_{19}^+ vibration of Tol-d_3, which was derived earlier from observed combination bands, results in a predicted wavenumber for the $(M_{19}^2)^+$ overtone of 732 cm^{-1}, which is reasonably close to the 739 cm^{-1} ZEKE feature assigned to the M_{10}^+ fundamental. The FWHM of this feature in the spectrum recorded *via* band O is ~19 cm^{-1}, which is considerably larger than that of the $(M_{18}M_{19})^+$ band in the same spectrum (~10 cm^{-1}), indicating the presence of at least two unresolved vibrations and hence supporting the overlap of these features in Tol-h_8, with the $(M_{19}^2)^+$ band likely being on the red side of the band.

The assignment of various other weak features in the REMPI spectrum was considered, and brief comments are now made on these. Two weak bands are observed for Tol-d_3 at 687.2 and 705.6 cm^{-1} assignable to the vibrations of the Tol-d_3–Ar complex which correspond to the transitions denoted O and P for bare Tol-d_3 (and are each labeled by the corresponding letter, with a bar over it). The same transitions for the Tol-h_8–Ar complex are not observed; however, these experiments were carried under different conditions. A weak band is observed at 863.2 cm^{-1} for Tol-h_8, which is assignable to the $M_{29}M_{30}$ combination vibration, consistent with the assignment of a feature observed at 864 cm^{-1} in the excitation spectrum reported by Hickman *et al.*[3] Another weak band is observed ~54.5 cm^{-1} above band M, with a second weak feature observed at the same wavenumber above N, consistent with transitions to the 3(+) torsional level of each of these two vibrations. Consistent with these assignments, weak bands observed at 743.2 cm^{-1} and 760.4 cm^{-1} for Tol-d_3 are assigned to the O[3(+)] and P[3(+)] vibration-torsion levels, respectively. See Table IV of Ref. 1 for torsional level wavenumbers. We note that the $m = \pm 3$ torsional levels mix to form new torsional states, which are symmetric and antisymmetric combinations of the $m = 3$ basis functions, which have a_1'' and a_2'' symmetry, respectively (G_{12} molecular symmetry group); these may be termed 3(+) and 3(−).[23]

(We note that in Ref. 1, we used the incorrect notation $m = +3$ and $m = -3$ to label these combinations, and we correct that here.)

Attempts were made to record time-resolved spectra of these Fermi resonances, but unfortunately they were just too far apart to allow simultaneous overlap within the 13 cm^{-1} wide ps pulse width and hence no coherent wavepacket could be prepared. As a consequence, SEVI spectra were recorded (but are not shown) with the excitation wavelength of the ps pulse tuned to overlap each feature separately in turn. As expected, the resulting tr-SEVI spectra exhibited no time dependence and simply resembled the ZEKE ones, albeit with slightly degraded resolution.

C. 880–1080 cm^{-1} region

The REMPI spectra recorded for this region for both Tol-h_8 and Tol-d_3 are shown in Figure 3(a).

1. Tol-h_8

The appearance of this region for Tol-h_8 agrees well with the LIF spectrum reported by Hickman *et al.*[3] in which two dominating vibrations were observed at 935 and 966 cm^{-1}, which were assigned as vibrations 10 and 11 in the notation employed therein, which correspond to the present M_8 and M_9 vibrations, respectively. These are in excellent agreement with the peak positions of 933.5 and 965.1 cm^{-1} observed in the present REMPI spectrum.

The ZEKE spectra for Tol-h_8, recorded *via* each of these two levels, are presented in the upper traces of Figs. 3(b) and 3(d). These are seen to be similar in appearance, with a very intense band observed in each spectrum, with peaks at 981 and 990 cm^{-1} in the spectra recorded *via* the M_8 and M_9 intermediate levels, respectively, which are easily assigned from the $\Delta v = 0$ propensity rule. The assignment of $M_8^+ = 980$ cm^{-1} is in excellent agreement with the weak band d assigned in our previous work;[1] similarly, the feature observed at 997 cm^{-1} in the M_8 ZEKE spectrum appears to correspond to the previously observed band e, assigned as the $(M_{11}^2)^+$ vibration.[1] (Both features were observed in the ZEKE spectra recorded via the two main components of the ~460 cm^{-1} Fermi resonance.) The width of the M_9^+ band, in Fig. 3(d) suggests that it consists of more than one component, it seems there could be an unresolved contribution from M_8^+ on the low wavenumber side, and it is also plausible that there is an unresolved contribution from $(M_{11}^2)^+$ on the high wavenumber side. On the other hand, no contribution of the M_9^+ vibration is evident in the obtained ZEKE spectrum when exciting via M_8. It seems that M_8 and M_9 are not in Fermi resonance in the S_1 state. Given the energetic proximity, it is interesting to note that these vibrations also do not seem to be coupled in the cation.

The M_8 and M_9 bands were too far apart to prepare these states coherently, although SEVI spectra (not shown) with no time delay were recorded. These closely resembled the ZEKE spectra, but with a degraded resolution. Meek *et al.*[8] report a MPI-PES spectrum recorded *via* M_8, in which progressions with spacings of ~480 and ~960 cm^{-1} are observed (note that a value of 940 cm^{-1} is given in Figure 2 of Ref. 8, but 960 cm^{-1} is given in the text), in reasonably good agreement with the values of 496 cm^{-1} determined for M_{11}^+ and 980 cm^{-1} for the M_8^+ vibration, determined in the present work and Ref. 1. In the publications of Meek *et al.*[8] and Whiteside *et al.*,[9] the spectra recorded via these intermediate levels have an unstructured spectrum, but with some structure retained in the spectrum when overlapped picosecond pulses are used.[9] This is at odds with the present ZEKE (and SEVI) spectra, and the dispersed fluorescence spectra[3] recorded *via* these intermediate levels, where the spectra are much cleaner and do not show a significant congestion of bands.

The feature observed at 915.5 cm^{-1} in the present work, has been previously assigned[3] to the $M_{12}M_{14}$ combination, based on activity in the DF spectrum, and this appears to have a counterpart at 912.7 cm^{-1} observed here in the corresponding spectrum of Tol-d_3. This is consistent with the small shifts of a_2 symmetry vibrations upon deuteration of the methyl group calculated (see Table I), and the wavenumber values are also consistent with the calculated values. Hickman *et al.*[3] suggested possible assignments for the bands observed in the excitation spectrum of Tol-h_8 reported in their work at 988 cm^{-1} and 997 cm^{-1}, to the FR components arising from the ZOSs $M_{11}M_{29}$ and $M_{19}M_{20}M_{29}$ – i.e., M_{29} in combination with each of the two most intense Fermi resonance components in Region A (at ~460 cm^{-1}, see Figure 1) arising from the ZOSs, M_{11} and $M_{19}M_{20}$; but these were not confirmed by DF spectroscopy. The relative intensities of these bands differ somewhat to those observed for the parent bands, as does the wavenumber separation; however, this may be an effect of the differing coupling strength between these vibrations, as observed for the vibration-torsion combinations of the same ZOSs, each with 3(+).[1,23] A possible alternative assignment for the band at 988 cm^{-1} is to the M_8 [3(+)] vibration-torsion level, with further weight added to this assignment by the observation of a band at 1019.9 cm^{-1}, which can be assigned to the M_9[3(+)] level: these both involve torsional levels which have been observed here for other vibrations of a_1 symmetry (also, see Ref. 1).

Two weak bands, denoted "y" and "z" in the ZEKE spectrum recorded *via* M_8 require assignment. Band y, which is observed at 1165 cm^{-1}, might be assigned to M_7^+ based on the calculated wavenumber for this vibration (see Table II); however, a feature at 1190 cm^{-1}, observed in a later ZEKE spectrum and discussed below, is assigned to that fundamental, which is in better agreement with the calculated value. Other possible assignments are the $(M_{11}M_{30}^2)^+$ combination or the $(M_{18}^2)^+$ overtone, each of which has calculated values in good agreement with the observed value. The observation of the former would suggest that the $(M_{30}^2)^+$ band should have been observed, but this lies outside of the region scanned. The better agreement of the $(M_{18}^2)^+$ calculated value leads us to favour this assignment at the current time. Symmetry-allowed assignments of band z at 1327 cm^{-1} include $(M_{14}^4)^+$ and $(M_{11}M_{29}M_{30})^+$ with the absence of the $(M_{29}M_{30})^+$ band at ~820 cm^{-1} perhaps favouring the first possibility, although the $(M_{14}^2)^+$ might then be expected, but is outside the scanned region. It is not possible to favour any one assignment strongly at the present time. Another

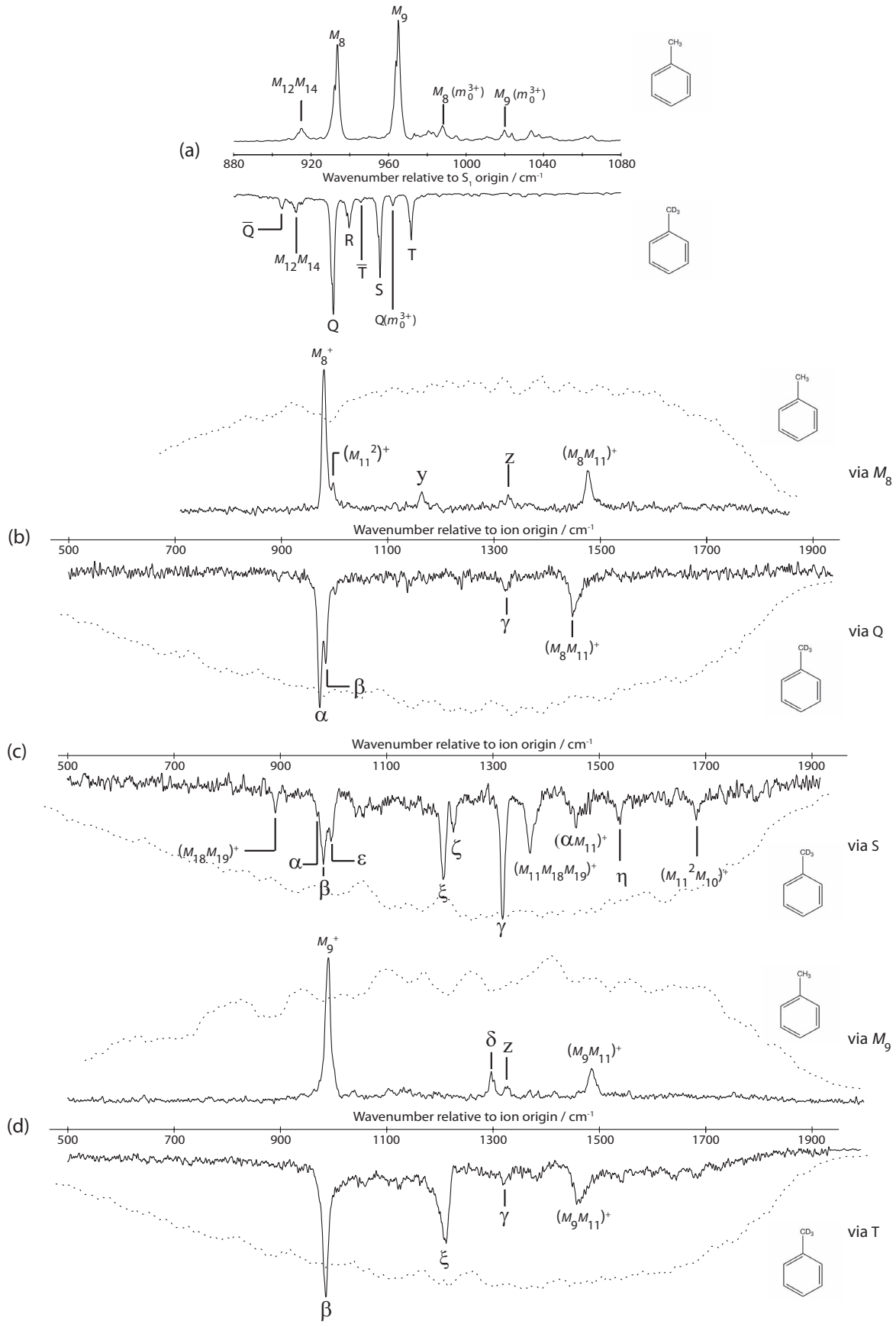

FIG. 3. (a) Expanded view of the (1 + 1) REMPI spectra of Tol-h_8 (upright) and Tol-d_3 in the range 880–1080 cm^{-1}. (b) contains the ZEKE spectra recorded *via* M_8 of Tol-h_8 and band Q of Tol-d_3, (c) contains ZEKE spectrum recorded *via* band S of Tol-d_3, and (d) contains ZEKE spectra M_9 of Tol-h_8 and band T of Tol-d_3. Spectra for Tol-h_8 and Tol-d_3 have been paired up based on their appearance and assignment: see text. The assignment of bands marked with letters is discussed in the text. The dotted lines indicate the intensity of the UV light across the region.

band is observed in the ZEKE spectrum recorded *via* M_9 at 1296 cm^{-1} and is denoted "δ." One possible assignment of this feature is to the $(M_{10}M_{19}M_{20})^+$ combination band; however, this has the weakness that the $(M_{19}M_{20})^+$ combination (at ~530 cm^{-1}), is not observed in this spectrum, although the UV intensity is weaker at the start of this wavenumber range. Another possibility is the $(M_{17}M_{18})^+$ combination of two b_1 symmetry vibrations, which has a calculated wavenumber in reasonable agreement with the observed one, and is currently favoured.

2. Tol-d_3

This wavenumber range of Tol-d_3 is considerably more complicated than that of Tol-h_8. In order to aid assignment of these vibrations, ZEKE spectra were recorded *via* bands labeled "Q," "S," and "T," in trace (a) of Figure 3, which occur at 931.9, 955.9, and 972.1 cm^{-1}, respectively. It is notable that there are two extra main features in the REMPI spectrum across this wavenumber range (bands Q, R, S, and T, *vs.* the M_8 and M_9 features), when compared to Tol-h_8. One obvious interpretation is that two ZOSs have shifted down in wavenumber in Tol-d_3 compared to Tol-h_8; however, there are no obvious features of this intensity slightly higher in wavenumber, in the Tol-h_8 REMPI spectrum. As such, we work on the hypothesis that two vibrations have shifted in wavenumber such that they are now in Fermi-resonance with M_8 and/or M_9. Further, a perusal of the calculated wavenumbers suggests that we do not expect either of these latter two vibrations to shift much between the two isotopologues. This does seem to be the case if band Q, at 931.9 cm^{-1}, is assigned to M_8 since the M_8 vibration has been assigned to the band at 933.5 cm^{-1} for Tol-h_8. On the other hand, no intense band in the Tol-d_3 REMPI spectrum appears as close to the Tol-h_8 M_9 vibration, suggesting that this vibration is now in Fermi resonance in Tol-d_3 and has hence shifted in value. We shall examine this in the below.

The ZEKE spectrum recorded *via* band Q closely resembles that recorded *via* the M_8 level of Tol-h_8, with an intense feature, band α, being observed at 974 cm^{-1}, which agrees favourably with the calculated wavenumber for Tol-d_3 M_8^+ (see Table II). The observed wavenumber would also be consistent with an assignment to $(M_{29}^2)^+$, however, this does not fit in with expectations based on the corresponding Tol-h_8 spectrum. Consequently, band Q is assigned to M_8 for Tol-d_3, consistent with the expected small shifts from the calculated wavenumbers, as noted above.

There is also a shoulder on the high wavenumber side of band Q in this ZEKE spectrum at 987 cm^{-1}, denoted β in the lower trace of Figure 3(b). This band dominates this wavenumber region when exciting via band T – see inverted trace of Fig. 3(d). A reasonable assignment of this feature is to the M_9^+ fundamental, based on the Tol-h_8 spectra and the good agreement with the calculated wavenumbers. This is initially a little unexpected since band S is more intense than band T and we would expect the more intense band to be the one that arose from a vibrational eigenstate that has the largest contribution from the ZOB and the "extra" bands in the Tol-d_3 spectrum would be expected to come from other vibrational eigenstates that arise from Fermi resonance, and so be of lower intensity; this will be discussed further below. That bands are in Fermi resonance, is supported by the same ZEKE bands being observed when exciting via different features, but with different relative intensities.

We now discuss the assignment of the intense band γ observed at 1318 cm^{-1} when exciting via S. If this arises from a $\Delta v = 0$ transition, then we require bands in the S_1 state that are in close energetic proximity to M_8 and M_9 and of the correct symmetry to interact; further, there would have to be a large shift in the vibrational wavenumber upon ionization, suggesting the involvement of vibrations of a_2 or b_1 symmetry, based on the trend of increasing wavenumber between the S_1 and D_0^+ electronic states for vibrations with these symmetries (see Ref. 2 and Table II). Hence, for example, we can dismiss the $(M_{14}^4)^+$ band (estimated position ~1336 cm^{-1}) as an assignment for γ since, although it has the correct symmetry, the S_1 value is far from the M_8 and M_9 positions. One possible assignment we have identified is that band γ arises from the $(M_{16}M_{19})^+$ combination vibration, which has a calculated wavenumber—see Table II—in good agreement with that of band γ. This combination also has the correct overall symmetry, and contains two vibrations of b_1 symmetry (and hence shifts significantly upon ionization). The calculated S_1 wavenumber is somewhat higher than the wavenumber of band S at 955.7 cm^{-1}; however, we also note that if this combination vibration is in Fermi resonance with M_9, then it will shift down in observed wavenumber; this would also be consistent with band T being at higher wavenumber than the M_9 band in Tol-h_8. It is also notable that, although band γ is only very weak in the ZEKE spectrum obtained when exciting via band T, band β appears strongly in both spectra. We conclude that the assignment of bands S and T are to vibrational states that arise from a Fermi resonance between $M_{16}M_{19}$ and M_9. The $M_{16}M_{19}$ vibration would appear above 1000 cm^{-1} in the REMPI spectrum for Tol-h_8, which would be one explanation as to why this vibration is not observed in this region for that isotopologue; but also this would be consistent with this band being "dark" and only observed in Tol-d_3 by virtue of the Fermi resonance with M_9. We reiterate that the stronger intensity of band S compared to band T is unexpected and that this will be discussed below. It is interesting to note that band γ appears weakly in the spectrum obtained when exciting via band Q, suggesting that M_8 may also be interacting weakly with $M_{16}M_{19}$; this is supported by the weak band α observed when exciting via S.

We now move onto the assignment of bands ξ and ζ in the ZEKE spectrum at 1211 cm^{-1} and 1227 cm^{-1}, respectively, observed most strongly when exciting via band S, but also seen strongly when exciting via band T. It is possible to come up with a number of assignments for ξ based upon the calculated vibrational values in Table II. For example, M_7^+ and the combination bands $(M_{17}M_{18})^+$ and $(M_{10}M_{11})^+$ each have reasonable calculated values, and each are of a_1 symmetry; however, neither of them have a corresponding S_1 value that suggests they would be coupled to M_9 or $M_{16}M_{19}$ (see above) and so these would be the result of Franck-Condon activity as a result of structural changes between the S_1 and D_0^+ states. One other possibility for the assignment of band ξ that

would be consistent with a ZOS that could be in Fermi resonance in S_1 is $(M_{15}M_{20})^+$, but $M_{15}M_{20}$ has a calculated scaled value somewhat lower than 1211 cm^{-1}, even though the anharmonic value is much closer. On the other hand, the calculated scaled S_1 wavenumber for $M_{15}M_{20}$ is in excellent agreement with the position of band R at 944 cm^{-1}. Further support for the involvement of $M_{15}M_{20}$ comes from the study of Butler *et al.*[24] on fluorobenzene. In that work a band at 922 cm^{-1}, previously assigned to M_7 was reassigned to the "apparently unlikely" $M_{15}M_{20}$ band on the basis of the dispersed fluorescence spectrum, and was deduced to be in Fermi resonance with M_8. Recalling our demonstration that there are strong similarities of the electronic spectra of the two toluene isotopologues to those of fluorobenzene and chlorobenzene,[1,2] then this concurrence of assignments lends weight to each. It is noteworthy, however, that bands ξ and ζ are not present in the ZEKE spectrum obtained when exciting via band Q, which was assigned to M_8 in the above. We conclude that the weak band R arises from a strong interaction between M_9 and $M_{15}M_{20}$. From this comparison, our favoured assignment for band ξ is to the $(M_{15}M_{20})^+$ combination. We note that there are weak features in the ZEKE spectrum at ~1150 cm^{-1} which may be attributable to the appearance of $(M_{15}M_{20})^+$, but this is far from definitive. It is interesting to note that there seems to be little or no interaction of M_8 with any other vibrations, including M_9, either in the S_1 state or in the ZEKE spectrum (see above). The ZEKE spectra obtained when exciting via band S additionally shows band ζ at 1227 cm^{-1}, where an assignment to M_6^+ seems reasonable from the calculated vibrational wavenumbers (see also later). There is also evidence for an unresolved feature on the low wavenumber side of band ξ in the ZEKE spectrum obtained when exciting via band T, which can be tentatively attributed to activity in M_7^+or $M_{17}M_{18}^+$.

Thus, it seems that bands R, S, and T are part of a complex Fermi resonance and this is supported by the appearance of bands β and γ in both recorded ZEKE spectra. That band γ appears weakly when exciting via bands Q and T, and very strongly via band S, suggests there may be some small interaction of M_8 in this region, but it must be very limited. Overall, it is difficult to unpick the whole picture of the vibrational coupling on the basis of these results, and recording a ZEKE spectrum via band R, as well as for other isotopologues, would provide additional and valuable insight into this spectral region. It is a shame that we did not attempt to record spectra via band R during these experiments, but this seemed too weak to attempt at the time. We may explore this further in the future, although this may require improvements to the sensitivity of our apparatus. We also note that, unlike the ZEKE spectra recorded *via* the M_8 and M_9 intermediate levels of Tol-h_8, the spectra recorded *via* bands S and T show a broad "hump" on which a structured spectrum is superimposed; no such hump is obvious when exciting via band Q. We shall comment on this below. A definitive assignment of band ε, at 985 cm^{-1} seen in the ZEKE spectrum recorded via band S is difficult, but we note that the $(M_{11}M_{19}M_{20})^+$ combination is expected to have a wavenumber of ~980 cm^{-1}. This would be consistent with the tentative assignments made to this wavenumber region of the Tol-d_3 cation in Ref. 1 and fits with experimental values determined in Ref. 1, as well as the calculated wavenumber values.

There are several other bands observed in the Tol-d_3 REMPI spectrum which require assignment. The weak feature at 905.1 cm^{-1} is likely due to a vibration of the toluene–Ar complex, which corresponds to that giving rise to band Q for bare toluene. Similarly, the very weak band at 945.1 cm^{-1} is assignable to the toluene–Ar complex vibration which corresponds to band T, with the corresponding toluene–Ar complex transition of S expected to be coincident with band Q. As we noted above, it just seems to have been "fortuitous" that the optimized conditions for the Tol-d_3 spectra also led to the production of toluene–Ar complexes. As with other vibrations of a_1 symmetry, the Q[3(+)] vibration-torsion is observed, with the corresponding vibration-torsion bands for the other main features seemingly being too weak to observe.

D. 1080–1450 cm^{-1} region

The REMPI spectra recorded for this wavenumber region are shown in Figure 4(a) for Tol-h_8 and Tol-d_3.

1. Tol-h_8

Concentrating initially on the Tol-h_8 spectrum in the upper trace, we can see that there is a clump of bands at ~1190 cm^{-1}, labeled Region D, which are reminiscent of the Fermi resonance at ~460 cm^{-1}. The difference in energy between this clump and the ~460 cm^{-1} FR is ~730 cm^{-1}, which is close to the wavenumber for the $M_{10}/M_{18}M_{19}$ Fermi resonance (see Table II and above). Hence, we initially anticipate that the features at ~1190 cm^{-1} may arise from eigenstates that arise from a "Fermi resonance of Fermi resonances." We refer to these eigenstates as A, B, C, and D at 460 cm^{-1}, and M and N at 730 cm^{-1}. Eigenstates A–D are made up of M_{14}^2, M_{11}, $M_{19}M_{20}$, and $M_{18}[3(-)]$ – see Refs. 1, 18, and 23 – and, although these are all mixed, eigenstate A is predominantly M_{14}^2, B and C are each mostly made up of significant contributions of M_{11} and $M_{19}M_{20}$, and band D is predominantly $M_{18}[3(-)]$. We have discussed eigenstates M and N in the above, and these are also made up of significant mixtures of two ZOSs: $M_{18}M_{19}$ and M_{10}.

The vibrational eigenstates of the 1190 cm^{-1} FR can now be viewed as combinations of the two original sets of FR vibrational eigenstates, and lead to eight possible combinations: vibrational eigenstates M and N, each in combination with vibrational eigenstates A, B, C, and D (where we are labeling the vibrational eigenstate by the same label as the band it gives rise to). Alternatively, in terms of the original ZOSs, these new combinations can be expressed as: $M_{14}^2M_{18}M_{19}$, $M_{11}M_{18}M_{19}$, $M_{18}M_{19}^2M_{20}$, and $M_{18}^2M_{19}[3(-)]$; and $M_{10}M_{14}^2$, $M_{10}M_{11}$, $M_{10}M_{19}M_{20}$, and $M_{10}M_{18}[3(-)]$ and the final vibrational eigenstates will be linear combinations of these. The calculated and expected experimental wavenumbers for these features are given in Table III in order of their S_1 wavenumber; it will be noticed that these suggest that the first four, lowest wavenumber, features are constituted predominantly of combinations of each of the ~460 cm^{-1} FR components with $M_{18}M_{19}$ and the next four,

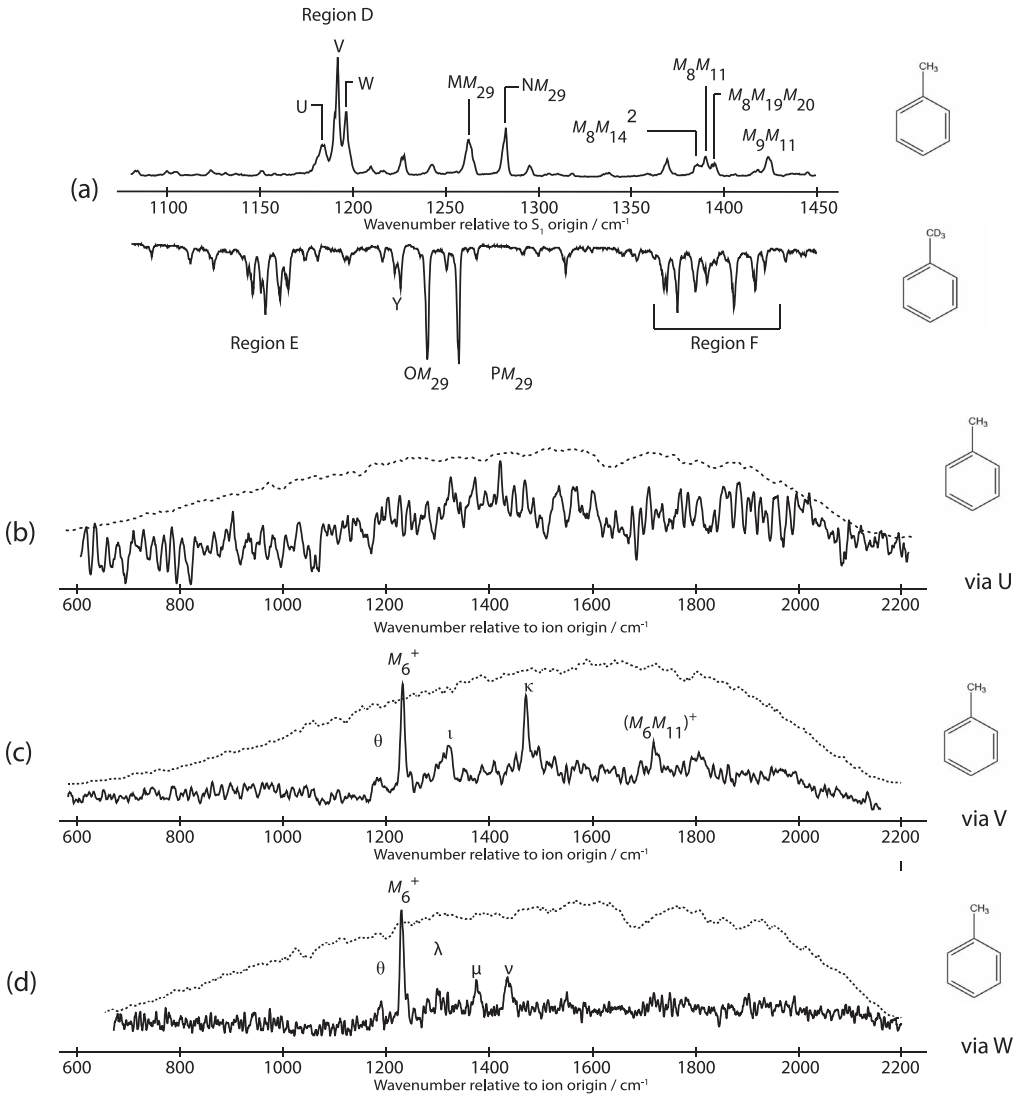

FIG. 4. (a) Expanded view of the (1+1) REMPI spectra of Tol-h_8 (upright) and Tol-d_3 in the range 1180–1450 cm^{-1}. Traces (b), (c), and (d) contain ZEKE spectra recorded *via* eigenstates U, V, and W, respectively. The assignment of bands marked with letters is discussed in the text. The dotted lines indicate the intensity of the UV light across the region.

highest wavenumber, features are constituted predominantly of combinations of each of the ∼460 cm^{-1} FR components with M_{10}. These values suggest that the intense bands U, V, and W at 1183.4, 1191.8, and 1196.2 cm^{-1} might be associated with the ∼460 cm^{-1} FR components in combination with eigenstate M, with the ∼460 cm^{-1} FR components in combination with eigenstate N appearing on the high wavenumber side to these features. Indeed, two weaker features to the blue of the main band at 1209.4 cm^{-1} and 1215.7 cm^{-1} could be associated with the combinations B+N and C+N, respectively (i.e., the two most intense features of the 460 cm^{-1} FR, in combination with eigenstate N). We note that the expected weak band arising from A+N could be contributing to the red side of the 1209.4 cm^{-1} feature, while the expected weak band arising from D+N could be part of the feature at 1226–1227 cm^{-1}, which seems to be comprised of two bands.

If the above assignments were correct, and bearing in mind the similar intensities of the two FR features at ∼730 cm^{-1}, the significant intensity differences of the two sets of features at ∼1190 cm^{-1} seems highly anomalous. A possible explanation comes from the DF fluorescence work of Hickman *et al.*[3] who report a DF spectrum from a feature at 1193 cm^{-1}, which would appear to be from the most intense band, band V. This spectrum was assigned as having a major contribution from M_6, but also showed significant IVR (to be discussed further below). Indeed, in our recent tr-SEVI paper,[10] we focused on the M_6 mode, and this will be referred to further in the below. If M_6 does contribute to this region and is coupled to the lower wavenumber vibrational eigenstates listed in Table II, then this could explain the higher intensities of the features arising from combinations of M + (A, B, C, and D). However, the appearance of the ∼ 1190 cm^{-1} feature is very similar to the one at ∼460 cm^{-1} and, even though this could be coincidental, the question arises as to why another vibrational eigenstate does not appear, owing to the additional contributing ZOS. A careful comparison of the FR features at ∼460 cm^{-1} and ∼1190 cm^{-1} reveals that band U is more intense and broader than is expected based on the 460 cm^{-1} FR,

TABLE III. Calculated wavenumbers for ZOSs of Tol-h_8 which are expected to have a composite value close to the position of the FR at ~1193 cm^{-1} and arise from combinations of the ZOSs that give rise to the vibrational eigenstates of the 460 cm^{-1} and 730 cm^{-1} FRs. Scaled values, obtained from 0.97× harmonic value (Table II), are given in parentheses and those derived from experimental values given in square brackets; the other values are the anharmonic values (see Table II). In all cases, the energy of the 3(−) levels have been taken from Table V of Ref. 1. The entries have been ordered in terms of their S_1 values. The letters are the band labels (see figures and text) and are also used for the corresponding vibrational eigenstates.[a]

		S_0	S_1	D_0^+
Band	Expected major contributions	Region A + band M combinations		
A	$M_{14}^2\ M_{18}\ M_{19}$	(1967)1997	(1169) [1186]	(1618) 1667 [1610]
B	$M_{11}\ M_{18}\ M_{19}$	(1672) 1704	(1201) [1191]	(1442) 1479 [1437]
C	$M_{18}\ M_{19}^2\ M_{20}$	(1827) 1863	(1207) [1197]	(1459) 1513 [1471]
D	$M_{18}^2 M_{19}$ [3(−)]	(1902) 1931	(1227) [1207]	(1554) 1606 [1559]
		Region A + band N combinations		
A	$M_{10}\ M_{14}^2$	(1584) 1604	(1165) [1205]	(1433) 1458 [1437]
B	$M_{10}M_{11}$	(1289) 1311	(1197) [1210]	(1257) 1270 [1264]
C	$M_{10}\ M_{19}\ M_{20}$	(1444) 1470	(1203) [1215]	(1274) 1304 [1298]
D	$M_{10}\ M_{18}$ [3(−)]	(1519) 1539	(1223) [1226]	(1369) 1397 [1386]

[a]Region A consists of four main bands, A, B, C, and D, with the compositions of A and D being mainly M_{14}^2 and M_{18}[3(−)], respectively; B and C are made up of significant amounts of both M_{11} and $M_{19}M_{20}$, with the majority contributions in that order (see Refs. 1, 18, and 23). Bands M and N have been deduced to be mixtures of $M_{18}M_{19}$ and M_{10}, with the majority contributions in that order (see main text). Thus, the calculated values are for the expected majority ZOS contributions, while the experimental values are obtained from adding the wavenumbers of the contributing vibrational eigenstates—these may shift slightly as a result of the interactions in this spectral region.

and therefore band U could contain a contribution from an additional unresolved vibrational eigenstate. At this point, it is useful to consider the ZEKE spectra and their assignment, before returning to this point. We have recorded ZEKE spectra, exciting separately through bands U, V, and W and we now discuss these.

As may be seen from Figure 4(b), the ZEKE spectrum obtained when exciting via feature U was structureless. As such, it made the reliable recording of this spectrum somewhat problematic, as our procedure for optimizing the ZEKE signal involves having the ionizing laser power high initially to obtain an electron signal, and then backing off on the power until the structured ZEKE spectrum appears (minimizing the production of "prompt" electrons formed by multiphoton processes, and the trapping of electrons by high ion densities). We then optimize the relative powers of the excitation and ionization lasers to obtain the highest quality ZEKE spectrum. When exciting via U, we initially had to carry out this procedure exciting through V or W to optimize the structured spectrum obtained (see below), and then scanning the excitation laser back to U and recording the ZEKE spectrum. In all cases, the spectrum was structureless, while returning back to V or W yielded a structured spectrum. Additionally, no subsequent optimization of the conditions when exciting through U yielded any clear structure. On the other hand, as is evident from Figures 4(c) and 4(d), excitation through V and W did yield a structured spectrum, albeit with an underlying broad background, and we now discuss these two spectra.

The most intense feature observed when exciting via V and W is a band at 1233 cm^{-1}, which matches well the calculated wavenumber for the M_6^+ vibration. This confirms that M_6 is a zero-order state contributing to the Fermi resonance at ~1190 cm^{-1} in agreement with the DF results,[3] and our recent time-resolved results.[10] Its intensity suggests it is a major contributor to the eigenstates giving rise to bands V and W. There are also a number of weaker features in the spectrum on top of the unstructured background, and we now consider their assignments.

We note that in the ZEKE spectrum obtained when exciting through V, there is a prominent feature, κ, at 1472 cm^{-1}. Using the calculated wavenumbers, we see that the best agreement is for the $(M_{18}M_{19}^2M_{20})^+$ combination, which is in near perfect agreement with the observed value. Note that we also see a band to higher energy at 1720 cm^{-1}, which matches the calculated position of the $(M_6M_{11})^+$ band very well. The observation of the latter is in line with the presence of the strong M_6^+ band, as combinations of fundamental vibrations with $M_{11}^{(+)}$ are prevalent in the electronic and photoelectron spectroscopy of monosubstituted benzenes; the absence of this band when exciting through W is slightly surprising (since a reasonably strong M_6^+ feature is present there also); however, we note that there is a significant unstructured background in this region, and there are inklings of some additional features.

Three other features appear clearly in the spectrum obtained when exciting via W, labeled λ, μ, and ν at 1299, 1375, and 1436 cm^{-1}, respectively. Band ν matches the expected position for $(M_{11}M_{18}M_{19})^+$, which is expected, based on the above comments. The wavenumbers of bands λ and μ match extremely well the expected positions for the combinations $(M_{10}M_{19}M_{20})^+$ and $[M_{10}M_{18}\ 3(-)]^+$, respectively; additionally, we note that the expected position for $(M_{10}M_{14}^2)^+$ coincides with that for $(M_{11}M_{18}M_{19})^+$, but the latter is expected to be the more intense, based on the S_1 intensities.

There are two other features in the ZEKE spectrum obtained when exciting via V: the broad band labeled ι, with a maximum at 1321 cm^{-1}, but with reasonable intensity extending to lower wavenumber, suggesting more than one contribution; and the weak feature, labeled θ, at 1190 cm^{-1}.

The broadband ι does not seem to come from any expected combination from the Fermi resonance, and so likely comes from other Franck-Condon-active bands, with the $(M_{16}M_{19})^+$ and $(M_{17}M_{18})^+$ combinations being possible, both being totally symmetric combinations of two b_1 modes. With this in mind, it is interesting to note that the $(M_{15}M_{19})^+$ combination is expected at 1437 cm^{-1}, and so may also be contributing to band ν. We note that band λ may also be contributing to the red side of band ι. Finally, we note that a less distinct feature is seen to the red of band λ, at ∼1280 cm^{-1}, that might be associated with $(M_{10}M_{11})^+$.

We now turn to the weak feature, band θ, which appears in the spectra obtained exciting via each of V and W: its wavenumber of 1190 cm^{-1} agrees very well with the expected wavenumber for M_7^+. However, the calculated value in the S_1 state suggests that M_7 is unlikely to be contributing significantly to the FR at ∼1190 cm^{-1}, and so we conclude M_7^+ is simply Franck-Condon active.

We note that it is possible to come up with other assignments of vibrations (overtones and combinations) with various torsional excitations in this wavenumber region (a number of which are discussed in Ref. 10), but we favour the assignments given, both on the grounds of their good match to the expected wavenumbers, but also owing to the majority being combinations involving the component vibrational eigenstates of the two prominent FRs at ∼460 and ∼750 cm^{-1}.

As noted above, it has been previously concluded that M_6 is involved in this FR feature,[3] and further that it is bright and carrying the majority of the intensity (i.e., it is a ZOB).[10] We have also seen that M_6^+ appears strongly in the ZEKE spectra via V and W, supporting this conclusion, but its contribution to band U is indeterminable from the unstructured ZEKE spectrum. It is therefore possible that band U contains a considerable contribution from M_6, and that severe mixing with a large number of ZOSs (dissipative IVR) has occurred. This is supported both by the structureless appearance of the ZEKE spectrum recorded when exciting at this wavenumber, and also the calculated S_1 wavenumber of M_6, which is in excellent agreement with that of band U. We conclude that the broadband U is associated with a significant number of ZOSs, but with a significant contribution from M_6, with M_6 also contributing a significant amount to the vibrational eigenstates that give rise to bands V and W. In addition, the ZOSs leading to the broadness and unstructured nature of the ZEKE spectrum of band U also contribute to bands V and W, causing the underlying broad background seen in their ZEKE spectra – see below for further discussion. The appearance of cation peaks corresponding to various expected combinations of the ∼460 cm^{-1} and ∼750 cm^{-1} FR eigenstates ties in with expectations, but the fact that there is very little overlap between the features seen when exciting via band V and W makes it difficult to make many definitive comments about the mixings between these. What is clear is that the eigenstates V and W (and likely U) each contain significant contributions from M_6. Additionally, eigenstate V also has a significant contribution from the combination of FR eigenstates C+N, as judged by the intensity of the $[M_{18}M_{19}^2M_{20}]^+$ band in the ZEKE spectrum. We note that this is wholly in line with the conclusion in Ref. 10 that $M_{18}M_{19}^2M_{20}$ is a doorway state for the transfer of energy from the ZOB M_6 to the bath of ZOSs in this region. We also note that the assignment of band λ is consistent with $M_{10}M_{19}M_{20}$ being another of the doorway states identified in Ref. 10. Notwithstanding the expected ordering of the combinations of the ∼460 cm^{-1} and ∼750 cm^{-1} FR eigenstates, the mixing of the contributing ∼460 cm^{-1} and ∼750 cm^{-1} FR vibrational eigenstates with M_6 is likely causing perturbations that would lead to resultant vibrational eigenstates with different energies. Thus, although the appearances of the FRs at ∼460 cm^{-1} and ∼1190 cm^{-1} are similar, this could be coincidental and the highly mixed nature of the vibrations in this narrow wavenumber range makes any detailed assignment of contributions, over and above the comments above, somewhat difficult. Clearly (at least), combinations of M_6 and the eight possible FR combinations are all likely to be present to some degree.

There are several other features in the (1 + 1) REMPI spectrum of Tol-h_8—see top trace of Figure 4(a)—which require assignment. Two reasonably intense vibrations are observed at 1262.1 cm^{-1} and 1282.5 cm^{-1}, which may be assigned to the combination of M_{29} and the components assigned to the $M_{18}M_{19}$ and M_{10} ZOSs [bands M and N – see Figure 2(a) of the Fermi resonance at ∼750 cm^{-1}]. These bands are labeled M+M_{29} and N+M_{29} in the upright trace of Figure 4(a) and are discussed further in Sec. III E. Corresponding features are observed at 1240.0 cm^{-1} and 1257.2 cm^{-1} in the Tol-d_3 spectrum, labeled O+M_{29} and P+M_{29}, respectively, in the inverted trace of Figure 4(a). (Both of these pairs of lines are themselves likely to arise from components of a Fermi resonance.) A triad of features, centred at ∼1390 cm^{-1}, is assignable to the M_8 vibration in combination with the components of the Fermi resonance at ∼460 cm^{-1}, which have been deduced to arise from the M_{14}^2, M_{11}, and $M_{19}M_{20}$ ZOSs (Refs. 1, 18, and 23); these higher-wavenumber vibrations are also likely in Fermi resonance.

2. Tol-d_3

We attempted to record ZEKE spectra for Tol-d_3 via many of the strong features of Region E—see inverted trace of Figure 4(a)—but none of these gave rise to a structured spectrum. However, we did succeed in obtaining tr-SEVI spectra, which clearly show structure at short time delays and have allowed the ZOB for Region E to be assigned to $M_{10}M_{11}$; this will be discussed further below. We first discuss the assignment of the resolved peaks in the complicated REMPI feature at ∼1150 cm^{-1}, shown in an expanded form in Figure 5. We note that the wavenumber of Region E is consistent with its being made up of vibrational eigenstates composed of those that give rise to "Region B" (the Tol-d_3 analogue of the ∼460 cm^{-1} FR feature in Tol-h_8), but now in combination with the components of the $M_{10}/M_{18}M_{19}$ FR, in a similar manner to the bands around ∼1190 cm^{-1} (Region D) in Tol-h_8. Hence, in the absence of further significant interactions (such as with another vibrational level), we would expect two sets of bands, resembling the bands in Region B, separated by about the same spacing as bands O and P. (Recall that the majority contributions of the vibrational eigenstates for Tol-h_8 and Tol-d_3 are reversed for the $M_{10}/M_{18}M_{19}$ pairs,

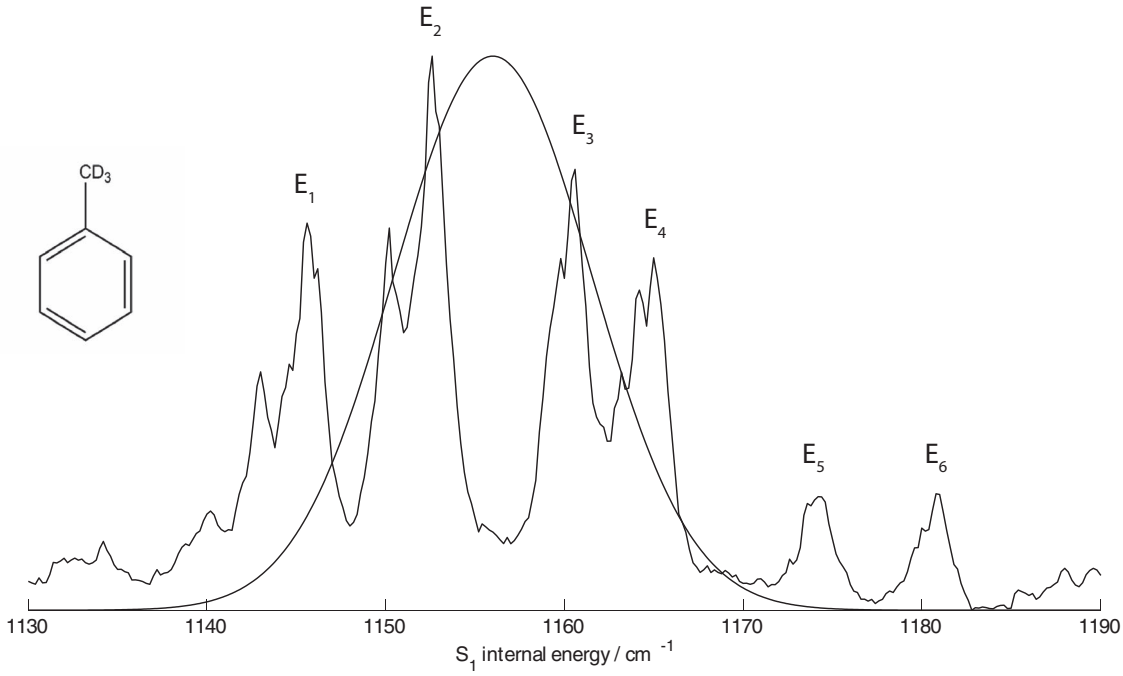

FIG. 5. Region E of the REMPI spectrum of Tol-d_3, showing an indication of the ps laser excitation pulse and hence the vibrational eigenstates excited.

if taken in wavenumber order.) The spectrum at ∼1150 cm^{-1}, at first sight, does not concur with this and hence we first calculate the expected wavenumbers of these combination features, and these are given in Table IV. We give most weight to the experimental values, which have been obtained by summing the experimental wavenumbers of the two contributing features to the combination. These, together with comparison with the appearance of Region B, suggest that the first three intense features, E_1, E_2, and E_3 at 1145.6, 1152.6, and 1160.6 cm^{-1} could have majority contributions from the three ZOSs $M_{10}M_{18}[3(-)]/M_{10}M_{11}$, $M_{10}M_{19}M_{20}$, and $M_{10}M_{14}{}^2$, respectively. The two weaker features to higher wavenumber, E_5 and E_6, at 1174.2 cm^{-1} and 1180.8 cm^{-1} may then have majority contributions from $M_{18}M_{19}{}^2M_{20}$ and $M_{14}{}^2M_{18}M_{19}$, respectively. The two other ZOSs expected, $M_{18}{}^2M_{19}[3(-)]$ and $M_{11}M_{18}M_{19}$ are expected to contribute to vibrational eigenstates that give rise to the 1165.0 cm^{-1} feature, E_4. Hence, Region E consists of a (very) complex Fermi resonance.

Note that, although we have discussed the involvement of the M_6 vibration for the ∼1190 cm^{-1} feature for Tol-h_8, in

TABLE IV. Calculated wavenumbers for ZOSs of Tol-d_3 which are expected to have a composite value close to the position of the FR at ∼1150 cm^{-1} and arise from combinations of the ZOSs that give rise to the vibrational eigenstates of the 460 cm^{-1} and 730 cm^{-1} FRs. Scaled values, obtained from 0.97× harmonic value (Table II), are given in parentheses and those derived from experimental values given in square brackets; the other values are the anharmonic values (see Table II). In all cases, the energy of the 3(−) levels have been taken from Table V of Ref. 1. The entries have been ordered in terms of their S_1 values. The letters are the band labels (see figures and text) and are also used for the corresponding vibrational eigenstates.[a]

		S_0	S_1	$D_0{}^+$
Band	Expected major contributions	Region B + band O combination		
E	$M_{10}\ M_{18}\ [3(-)]$	(1457) 1479	(1154) {1149}	(1275) 1309 {1281}
F	$M_{10}M_{11}$	(1241) 1262	(1154) {1151}	(1203) 1216 {1214}
G	$M_{10}\ M_{19}\ M_{20}$	(1385) 1410	(1164) {1156}	(1232) 1265 {1247}
H	$M_{10}\ M_{14}{}^2$	(1558) 1583	(1138) {1165}	(1407) 1442 {1410}
		Region B + band P combinations		
E	$M_{18}{}^2M_{19}\ [3(-)]$	(1836) 1864	(1161) {1166}	(1434) 1489{1433}
F	$M_{11}\ M_{18}\ M_{19}$	(1620) 1647	(1161) {1167}	(1362) 1396 {1366}
G	$M_{18}\ M_{19}{}^2\ M_{20}$	(1764) 1795	(1171) {1173}	(1391) 1445 {1399}
H	$M_{14}{}^2\ M_{18}\ M_{19}$	(1937) 1968	(1145) {1182}	(1566) 1622 {1562}

[a]Region B consists of four main bands, E, F, G, and H, with the compositions of E and H being mainly $M_{18}[3(-)]$ and $M_{14}{}^2$, respectively; F and G are made up of mixtures of M_{11} and $M_{19}M_{20}$, with the majority contributions in that order (see Ref. 1). Bands O and P have been deduced to be mixtures of M_{10} and $M_{18}M_{19}$, with the majority contributions in that order (see main text). Thus, the calculated values are for the expected majority ZOS contributions, while the experimental values are obtained from adding the wavenumbers of the contributing vibrational eigenstates—these may shift slightly as a result of the interactions in this spectral region.

our previous work[10] we have concluded that the M_6 ZOS is expected to blue shift by ~20 cm^{-1} on moving from Tol-h_8 to Tol-d_3, and so is associated with one of the bands labeled Y in the inverted trace of Figure 4(a). On the other hand, other vibrations are expected to show significant red shifts (see Table II) when the methyl group is deuterated.

The tr-SEVI spectra were obtained by positioning the laser pulse at 1156 cm^{-1} (see Figure 5), so that there was good overlap with the most intense bands of the feature referred to as Region E. Spectra were recorded at a number of time delays from 0 to 500 ps and are shown in Figure 6. As may be seen, at long delays essentially all structure is lost, consistent with the unstructured ZEKE spectra which are recorded with nanosecond lasers—this is consistent with dissipative IVR. As mentioned earlier, at 0 ps a structured spectrum is obtained. At time delays up to 20 ps, band intensities are seen to be oscillating in intensity, indicating that there is strong coupling between the bright state and at least one doorway state; thus, we are in the intermediate IVR regime here. The strongest peak in the tr-SEVI spectrum at 0 ps is measured to be at ~1200 cm^{-1} which, within the error of our SEVI measurements is consistent with the expected position of $(M_{10}M_{11})^+$, from both the calculated vibrational wavenumbers, and its position in the ZEKE spectrum recorded via O, and hence this allowed the ZOB to be assigned to $M_{10}M_{11}$. Consistent with the appearance of bands that involve $M_{11}{}^+$, we note there are bands at one quantum above and below, namely, the band at ~740 cm^{-1} may be assigned to $M_{10}{}^+$ and the band at ~1660 cm^{-1} may be assigned to $(M_{10}M_{11}{}^2)^+$; both of these additional bands vary in intensity in the same way as $(M_{10}M_{11})^+$. Other bands are varying in intensity in a different way, and we will come back to these shortly. First, we note that we can ascertain the time dependent behavior of the ZOB, $M_{10}M_{11}$, by monitoring the intensity of the $M_{10}{}^+$ feature at ~740 cm^{-1} as this was in a clean region of the spectrum, and allowed the intensity variation to be followed to longer times, when the broad underlying background obscured the main $(M_{10}M_{11})^+$ band. We have plotted this variation in

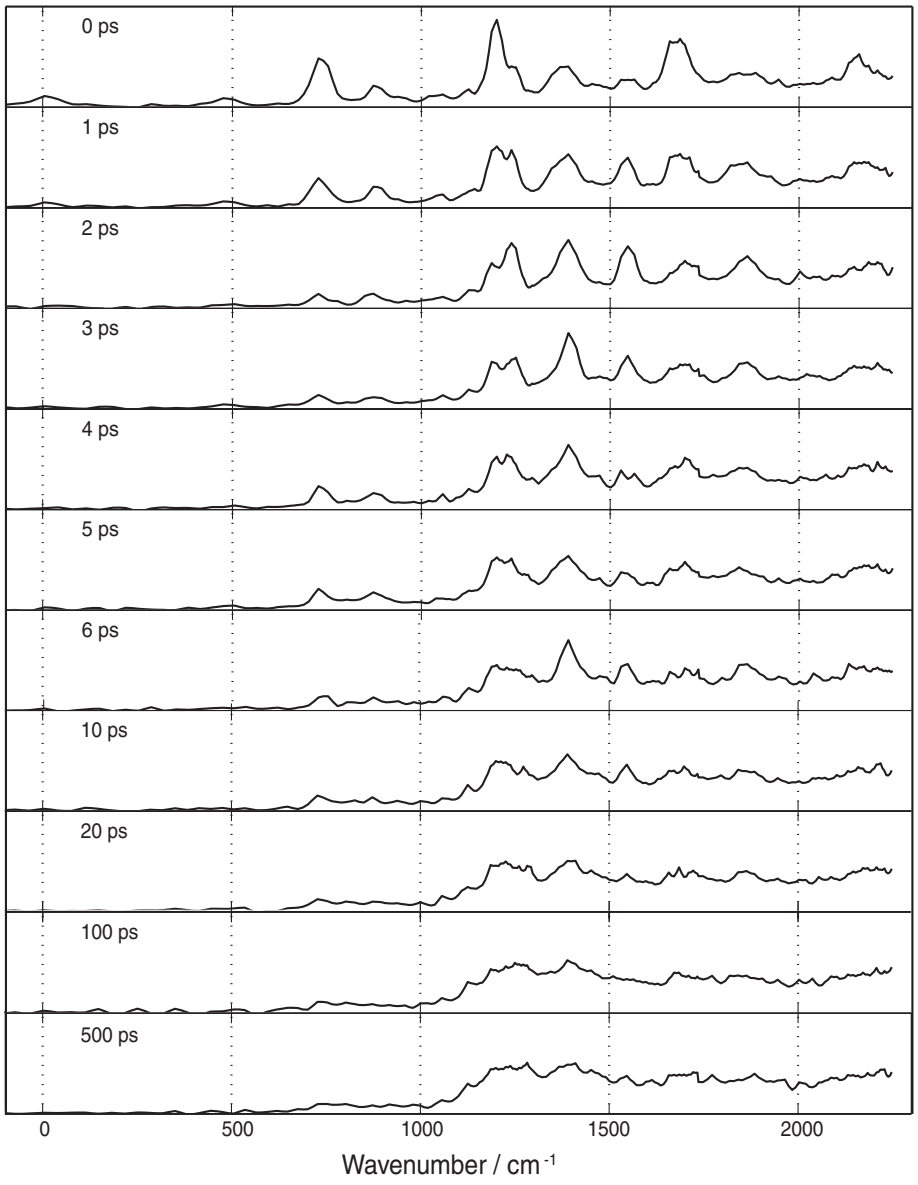

FIG. 6. tr-SEVI spectra recorded using the excitation indicated in Figure 5, at different time delays.

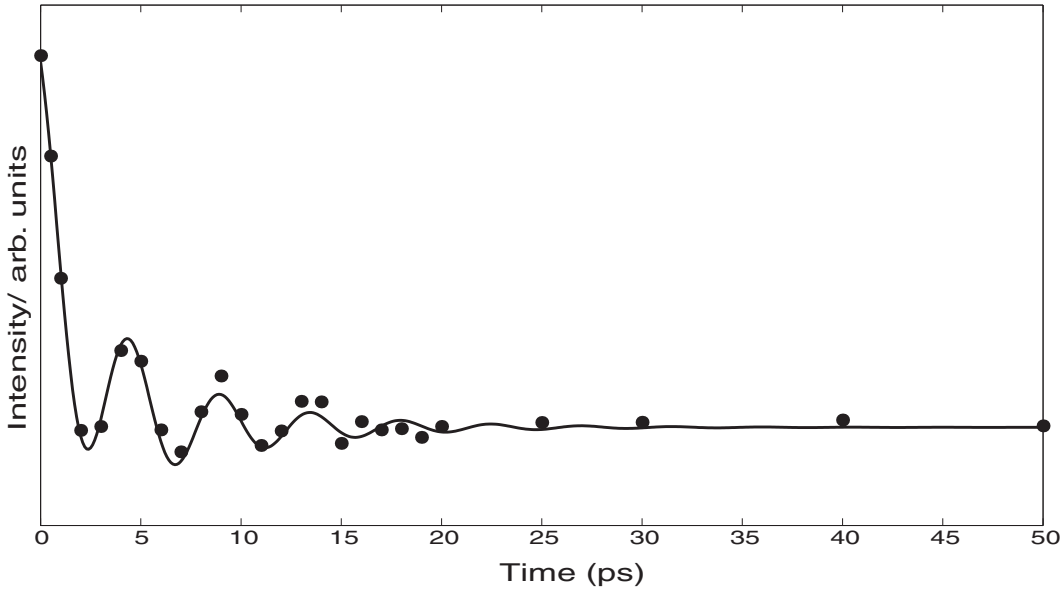

FIG. 7. Trace showing the intensity variation of the M_{10}^+ band in the tr-SEVI spectrum with time. The dots are the experimental data points, while the line is obtained from fitting the data to Eq. (1).

intensity as data points in Figure 7; also shown in that figure is a fit to this data using the empirical equation (see Ref. 19 for further details)

$$I(t) = A + B\exp\left(\frac{-t}{\tau_1}\right) + C\exp\left(\frac{-t}{\tau_2}\right)\cos\left(\frac{2\pi t}{\tau_C}\right). \quad (1)$$

The best fit yielded $A = 24.0$, $B = 32.4$, $C = 16.5$, $\tau_1 = 1.7$ ps, $\tau_2 = 16.5$ ps, and $\tau_C = 4.5$ ps. This formula is appropriate for IVR involving one bright state, one strongly coupled doorway state, and many weakly coupled bath states. The value of τ_C allows the wavenumber separation of the states to be deduced as 7.4 cm^{-1}, which is consistent with both the separations of the more intense features at 1160.6 cm^{-1} and 1152.6 cm^{-1} as well as between the same 1160.6 cm^{-1} band and the one at 1145.6 cm^{-1}.

Looking back at the tr-SEVI spectra, we see that some bands are moving out of phase with the ~1190 cm^{-1} band, namely, one at ~1230 cm^{-1} and one at ~1540 cm^{-1}. Looking at the values in Table IV, it seems most likely that the ~1230 cm^{-1} SEVI band is due to $(M_{10}M_{19}M_{20})^+$, and hence is a dark state coupled to $M_{10}M_{11}$ in the S_1 state. This is interesting as it mimics the behavior shown for Tol-h_8 for the FR at ~460 cm^{-1} (see Refs. 1 and 23, and particularly Ref. 18). We note that the ~880 cm^{-1} band can be assigned as $(M_{18}M_{19})^+$ and it is interesting to note that this is present at $t = 0$, as is a band at ~480 cm^{-1}, which can be assigned to $M_{11}{}^+$, suggesting that the associated ZOS, $M_{11}M_{18}M_{19}$ has some bright character. The appearance of these bands, suggests that the $(M_{11}M_{18}M_{19})^+$ band should be present, and indeed the values in Table IV suggest that the band at ~1370 cm^{-1} can be assigned to this vibration; this band is present at 0 ps, but then increases in intensity further; this may be a result of the $M_{11}M_{18}M_{19}$ vibration being made up of a combination of a bright (M_{11}) and a (mostly) dark ($M_{18}M_{19}$) vibration. The band at ~1560 cm^{-1} is clearly a dark state and an obvious assignment is to $(M_{14}{}^2M_{18}M_{19})^+$ based on the calculated values in Table IV; however, it is surprisingly intense, given the weakness of the corresponding feature in the REMPI spectrum (at 1180.8 cm^{-1}). Although other features are present in the spectrum, these are weak and/or overlapped heavily making it difficult to distinguish them.

Similar observations for Tol-d_3 regarding the complexity of region E may be made regarding Region F (see Figures 1 and 4, inverted traces), which by comparison with the Tol-h_8 spectrum, is expected to consist of combination bands formed between the vibrations of the Fermi resonance at ~440 cm^{-1} (see Ref. 1) and the intense bands at ~950 cm^{-1}, which were themselves assigned to a number of ZOSs (see above). We did not attempt to record ZEKE spectra via any of these features.

Finally, we note that we have already mentioned the appearance of the combination bands M_{29}+O and M_{29}+P in Subsection III D 1, which refer to the combination of M_{29} with the FR components arising from the $M_{18}M_{19}$ and M_{10} ZOSs.

E. Additional tr-SEVI results

tr-SEVI spectra were recorded for Tol-h_8 via the two features at 1263 cm^{-1} and 1284 cm^{-1}, assigned as Fermi resonance component $M_{29}(M_{10}/M_{18}M_{19})$ (see Figure 1), in agreement with Ref. 3. As before, it was not possible to excite these two features coherently, since they are too widely spaced. From our discussion earlier, we concluded that M_{10} is a ZOB, and so in the present case, we would expect $M_{10}M_{29}$ to be the ZOB, and $M_{18}M_{19}M_{29}$ to be the ZOD. The wavelength of ps pump laser pulse was tuned to excite each vibrational band in turn and the resulting 0 ps SEVI spectra (not shown) were found to be similar to the SEVI and ZEKE spectra recorded for the $M_{10}/M_{18}M_{19}$ Fermi resonance components but with the most intense SEVI peaks shifted higher in wavenumber by ~486 cm^{-1}, which confirms their assignments as $(M_{29}M_{10})^+$

and $(M_{29}M_{18}M_{19})^+$. The relative intensities of these peaks indicated that the lower wavenumber REMPI feature at 1263 cm^{-1} contains a majority contribution from the $M_{29}M_{18}M_{19}$ ZOD while the feature at 1284 cm^{-1} contains a majority contribution from the $M_{29}M_{10}$ ZOB. This is the same energy ordering that was observed for the $(M_{10}/M_{18}M_{19})$ Fermi resonance doublet at ~750 cm^{-1}, for which the higher wavenumber component N contained a larger contribution from the M_{10} ZOB. Recording SEVI spectra as a function of time delay via the REMPI features at 1263 cm^{-1} and 1284 cm^{-1} showed that the SEVI band corresponding to the ZOB simply decayed with time in each case, and there were no oscillations in intensity; concurrently, regions of the spectrum that were dark initially, gained intensity over a broad region with time delay. Thus, there is rapid dissipative IVR for these features, indicating that each REMPI feature contains multiple eigenstates that are composed of coupled vibrational states. This is in contrast to the $M_{10}/M_{18}M_{19}$ Fermi resonance components at ~744 cm^{-1}, where the lack of time dependence in the SEVI spectra indicated that each REMPI feature contained a single vibrational eigenstate. The IVR time constants were measured to be 21 ± 5 ps for the REMPI band at 1263 cm^{-1} assigned to $M_{29}M_{18}M_{19}$ and 39 ± 11 ps for the REMPI band at 1284 cm^{-1} assigned to $M_{29}M_{10}$. This conclusion fits with the structureless spectra reported by Hickman *et al.*,[3] and we would anticipate largely structureless ZEKE spectra in this case. No corresponding spectra for Tol-d_3 were recorded.

Similar results were obtained when exciting through the band assigned as M_8M_{29}, which is located at ~1463 cm^{-1} for Tol-h_8 and ~1459 cm^{-1} for Tol-d_3, and the band at 1494 cm^{-1}, assigned as M_9M_{29} for Tol-h_8 (the corresponding Tol-d_3 band was not studied). In all cases, exponential decay of the $\Delta v = 0$ SEVI band was observed, and a corresponding growth of the "dark" region of the spectra. For M_8M_{29}, Tol-h_8 had an IVR time constant of ~35± 6 ps, while Tol-d_3 had a value of ~52 ± 6 ps. For M_9M_{29}, Tol-h_8 had an IVR time constant of 18 ± 6 ps.

F. IVR and the broad spectral background

1. General

As has been noted in the above, several of the ZEKE spectra for Tol-h_8 and Tol-d_3 demonstrate a broad underlying background. In the extreme, such as exciting via band U for Tol-h_8 or features within Region E for Tol-d_3, there do not appear to be any structured peaks; while in other cases, structured peaks appear on top of the broad background. Such broad backgrounds have been seen previously, in both REMPI-PES[9] and in dispersed fluorescence of toluene.[3] From quite early on, these broad backgrounds for toluene have been associated with IVR processes;[25] in particular, with wide-scale mixing between a significant number of contributing ZOSs in the S_1 state. This leads to a vibrational eigenstate that describes a wide range of motions such that fluorescence or ionization occurs to a wide range of vibrational levels; the number of these is such that almost all structure is lost in the spectrum, owing to the number of overlapping ZOS spectra. If all structure is lost, then in the time-resolved picture, this situation is consistent with the so-called dissipative IVR regime, whereby the number of coupled ZOSs is such that the energy in the ZOB state is rapidly redistributed to a large number of ZOSs and the number is such that the chances of a recurrence of the energy solely in a bright state is negligible. It seems clear that, at sufficiently high wavenumber, the dissipative picture will always dominate; however, for some of the spectra recorded via lower wavenumber S_1 vibrational states, it is perhaps surprising that structure is completely lost. Additionally, we note that the lack of structure when exciting via one band does not imply a loss of structure for all bands to higher wavenumber, as exemplified by our spectra. Thus, in line with one of the key conclusions of our previous paper,[10] the onset of wide-ranging IVR seems to be mode-specific, and occurs when particular states (so-called doorway states) are accessed that provide an efficient coupling mechanism to the bath of vibrational states whose number is continually increasing with wavenumber. Particularly at low wavenumber, the observation of doorway states relies on its energetic coincidence with a bright state. (Clearly, at much higher wavenumber, it is expected that there will be more and more "doorway" states coupled to the increasing bath of states as the numbers of overtones and combination vibrations builds up; and sufficiently high in wavenumber it is likely that essentially all states will become coupled to the bath via some mechanism.) It also seems clear that, lower down in wavenumber, the presence of low-frequency modes (vibrations/torsions) will serve to heighten the chance of coupling a doorway state to the increasing bath of states, owing both to the occurrence of a larger number of eigenstates formed from the various combinations and also by the provision of other coupling pathways; however, at low wavenumber it is still going to be critical that a doorway state exists that can couple a bright state to the bath. One of our groups has identified doorway states in both pFT and toluene,[10,19] mainly using time-resolved SEVI spectroscopy; we shall refer to the toluene work of previous studies and the present work further in the below. We will break our discussion down to consider the various wavenumber regions.

2. 730 cm^{-1} FR

We have discussed the assignment of the ZEKE spectra that are presented in Figure 2 for excitation through the two components of the Fermi resonances at ~730 cm^{-1} for both Tol-h_8 and Tol-d_3. As noted, the ZEKE spectra support the conclusions of Hickman *et al.*[3] with regards to the contributing ZOSs being M_{10} and $M_{18}M_{19}$ since the spectra show contributions from each of the corresponding cation vibrations, and these are well separated in wavenumber. In our work on the ~460 cm^{-1} FR in toluene,[1,18] we were able to make deductions about the contributions of each ZOS to the FR, and these were broadly in line with similar conclusions reached by Gascooke and Lawrance.[23] In the present case, this proves not to be so straightforward, with the appearances of the REMPI and ZEKE spectra apparently giving contradictory information. The REMPI spectra clearly show that for both isotopologues, the higher wavenumber feature is the more

intense, and hence would have a majority contribution from the ZOB. For Tol-d_3, the ZEKE spectra indicate this feature has a majority contribution from $M_{18}M_{19}$, while the lower wavenumber one has a majority contribution from M_{10}. On the other hand, the spectrum recorded for Tol-h_8 via feature M indicates that it has a majority contribution from $M_{18}M_{19}$, with the spectrum via N indicating more or less equal contributions. Furthermore, the 0 ps SEVI spectrum measured via feature N indicates a majority contribution from M_{10}. The conclusion that band M has a majority contribution from $M_{18}M_{19}$ would suggest that M_{10} is the ZOB in Tol-h_8, in line with the REMPI intensities. For Tol-d_3, however, the REMPI intensities would suggest that the higher wavenumber band is the ZOB, but the ZEKE intensities suggest this is $M_{18}M_{19}$. It does not appear to be likely that the ZOB is changing between the isotopologues.

A possible explanation of this is as follows. For Tol-h_8, although the calculated vibrational wavenumbers suggest that the $M_{18}M_{19}$ combination should have a higher value than that for M_{10}, these values are very close and deficiencies in the computational approach, such as neglect of anharmonic effects may change the order of these, so some caution is merited. Referring to the excitation spectrum of fluorobenzene,[24] we note that this FR is present there also, and assigned to the same pair of ZOSs. The lower component is the more intense and has been assigned as consisting of a majority contribution from M_{10}, based on the activity observed in the DF spectrum. Similar observations of activity have been made by Hickman *et al.*[3] for Tol-h_8, when exciting the higher wavenumber component, also assigned to M_{10}. Consequently, the experimental evidence points to band N having a majority contribution from M_{10} and with M_{10} being the ZOB. We cannot rule out $M_{18}M_{19}$ also having some bright character, since we were unable to excite the FR coherently. Hence, we suggest that M_{10} and $M_{18}M_{19}$ are very energetically close ZOSs and then Fermi resonance leads to the resulting vibrational eigenstates becoming separated in wavenumber. These conclusions are then in line with the DF, REMPI, ZEKE, and SEVI results for Tol-h_8.

We are still left with the slightly puzzling results from Tol-d_3. The ZEKE spectra and calculations are both consistent with the ordering of the ZOSs being reversed from that in Tol-h_8, and so the vibrational eigenstates would be expected to have reversed majority contributions; however, the REMPI spectra have bands that are quite close to being equal. We conclude that the intensities of the REMPI features are each affected by dissipative IVR effects to differing extents. Indeed, to be consistent with the ZEKE spectra, band O would be expected to be more intense than band P. We note that there are broad features in the spectrum around these two bands, and so we hypothesise that either the M_{10} vibration is itself coupled efficiently to the bath of dark states, or the lower of the two vibrational states formed after M_{10} and $M_{18}M_{19}$ couple becomes more efficiently coupled to the bath than does the higher wavenumber one. In conclusion, the above analysis suggests that the ordering of the ZOSs has reversed between Tol-h_8 and Tol-d_3, but that M_{10} is the ZOB in both cases.

We note that Whiteside *et al.*[9] observed broad photoelectron spectra with little structure when (likely) exciting through band N, at odds with the present ZEKE and previous DF results. One explanation for this would be that the beam conditions were warmer in those experiments, opening up the possibility of other IVR coupling mechanisms via Coriolis or vibration-torsion couplings via excited torsional levels.

3. M_8 and M_9

At around 950 cm^{-1}, there is a pair of bands for Tol-h_8 that have been assigned to M_8 and M_9, which we have concluded are not in Fermi resonance. On the other hand, for Tol-d_3, there are more bands, suggestive of vibrational features having moved into resonance with one or more of M_8 and M_9. As we noted above, it was not possible to excite these coherently and so no time-resolved results have been obtained. In any case, for Tol-h_8, we have noted that M_8 and M_9 do not appear to be in Fermi resonance. On the other hand, for Tol-d_3, there are extra bands which we have concluded arise from other vibrations coming into the vicinity of M_8 and M_9 and then interacting with them. We have concluded that M_8 does not seem to be strongly coupled to the interloping ZOS, and that it is M_9 that couples to give these new states intensity. The latter is confirmed by the essentially similar wavenumbers for the M_8 vibration in both Tol-h_8 and Tol-d_3, while the Tol-d_3 bands are all shifted from the position of M_9; and also the fact that when exciting via band Q (assigned to M_8) there is no obvious broad background to the ZEKE spectrum, while those recorded via T and S do show such a background. The ZEKE spectra indicate band T has the majority contribution from M_9, even though it is not the most intense, while bands R and S arise from Fermi resonance with M_9. As with the ~730 cm^{-1} features just discussed, we believe the expected REMPI intensities are affected by IVR, and it is clear from the ZEKE spectra in Figure 3 that there is more IVR for Tol-d_3 than there is for Tol-h_8. If M_9 is the doorway state for Tol-d_3 to the bath of ZOSs, then this would explain the reduced intensity of band T from that expected, even though it contains the largest contribution from the M_9 ZOB, and the broad background observed when exciting via T and S, but not from Q.

4. 1190 cm^{-1}(Tol-h_8) and 1150 cm^{-1}(Tol-d_3) FRs

In the above, we have discussed these two FR regions for Tol-h_8 and Tol-d_3, respectively. These are particularly noteworthy because of their very different nature, even though the majority of the contributing ZOSs are very similar in each case. Recall that in these regions we expect the FRs in Regions A and B to appear in combination with each of the FR components at ~730/750 cm^{-1}. In the absence of any other effects, we would therefore expect a pair of features, resembling the Regions A and B FRs, roughly separated by 20 cm^{-1}. However, for Tol-h_8 we find one intense set of features to lower wavenumber and a much weaker set to higher wavenumber, with the features in about the expected positions. Together with previously published tr-SEVI results and DF results, the explanation for this large intensity difference in Tol-h_8 can be attributed to the coincidental presence of M_6 in this spectral region. This bright state gives significant intensity to those components that are directly coupled to

$M_{18}M_{19}$. As such, when exciting through bands V and W, an intense M_6^+ band appears in the ZEKE spectrum. Unexpectedly, a clear contribution from another vibrational eigenstate does not appear in the REMPI spectrum, and again the explanation appears to rest with significant coupling to a bath of ZOSs that reduces the intensity of band U, which is also deduced to contain a significant contribution from the ZOB, M_6, supported by the fact that the calculated S_1 wavenumber is in very good agreement with the wavenumber of this feature. The significant coupling of the ZOSs that give rise to band U with the vibrational bath in this region is supported by the lack of structure in the ZEKE spectrum, plus the loss of intensity of the M_6^+ feature in the tr-SEVI spectra at long times.

Somewhat surprisingly, the Tol-d_3 spectrum shows very different behavior. First, the strong features in Region E are not associated with M_6, since this blue shifts, and so is too far away in wavenumber to contribute.[10] The tr-SEVI spectra indicate that in fact $M_{10}M_{11}$ is the bright state, notwithstanding the weakness of this state in the Tol-h_8 spectrum. The tr-SEVI spectrum does not show any evidence of any other bright state contributions, and so it is surprising that Region E is so intense, as is the fact that the bands marked Y, assigned as involving M_6 in Tol-d_3, are somewhat weak; particularly given the very bright nature of M_6 in Tol-h_8. We currently have no explanation for this dramatically different behavior of the combination bands involving M_{10} between the two isotopologues.

We note that for Tol-h_8 we have considered in depth that a potentially much tidier assignment would be that the eigenstates with majority contributions from M_{10} and $M_{18}M_{19}$ are the same way around in Tol-h_8 and Tol-d_3, with the strong ZEKE band seen when exciting via bands V and W then being assignable to $(M_{10}M_{11})^+$. In turn, this would lead to the conclusion that the bright state was the same vibration in both isotopologues, and further, it would be the one that is the ZOB in both contributing FRs. However, the expected wavenumber for $(M_{10}M_{11})^+$, based on our previous[1] experimental determination of the contributing vibrations, and its observation at 1269 cm^{-1} when exciting via band N in the present work, makes it clear that the strong feature cannot be $(M_{10}M_{11})^+$, but must be assigned to M_6^+ based on the calculated wavenumber, the DF results and the tr-SEVI spectra.

Finally, we note that we have recorded tr-SEVI spectra of several other higher wavenumber features, which show dissipative IVR, with the rate of IVR higher for the higher wavenumber features. Additionally, the IVR rate might be expected to be higher for Tol-d_3 than Tol-h_8; however, it was measured to be slower via the M_8M_{29} feature in line with comment made in Ref. 10 that the higher density of states in Tol-d_3 does not necessarily lead to enhanced IVR. Overall, there does seem to be a general, but not monotonic, trend for increased rates of dissipative IVR with increased density of states at sufficiently high wavenumber; however, this is only a very limited dataset. To lower wavenumber, however, it is clear that whether IVR is dissipative or not depends critically on there being both a sufficiently dense set of ZOSs available for coupling, but also that there is an available state that can mediate the coupling of the ZOB to the bath of ZOSs – a doorway state. It is also possible, higher in wavenumber, for there to be states that can still show no IVR or restricted IVR (Fermi resonance) if there is no doorway state available to provide the coupling route.

TABLE V. Assigned bands observed in the 1 + 1 REMPI spectra of Tol-h_8 and Tol-d_3. A···B indicates two levels that are in Fermi resonance.

	Wavenumber/cm^{-1}	
Assignment	Toluene-h_8	Toluene-d_3
$M_{20}{}^2$	289.9	268.9
$M_{30}{}^1$	331.4	294.6
$M_{14}{}^1\,M_{20}{}^1$	371.0	359.2
Tol-Ar$M_{11}{}^1$	431.0	412.2
$M_{14}{}^2$	451.8	452.4
$M_{11}{}^1\cdots M_{19}{}^1\,M_{20}{}^1$	456.6	437.8
$M_{19}{}^1\,M_{20}{}^1\cdots M_{11}{}^1$	462.2	443.0
$M_{18}{}^1[3(-)]$	472.6	436.0
$M_{14}{}^2\,[3(+)]$	…	480.6
Tol-Ar$M_{29}{}^1$	504.9	501.3
$M_{11}{}^1\,[3(+)]$	512.9	…
$M_{29}{}^1$	531.3	529.1
$M_{14}{}^1\,M_{19}{}^1$	539.3	530.5[a]
$M_{19}{}^2$	628.5	612.3
$M_{16}{}^1$	696.8	688.0
$M_{18}{}^1\,M_{19}{}^1\cdots M_{10}{}^1$	734.4	729.6
$M_{10}{}^1\cdots M_{18}{}^1\,M_{19}{}^1$	753.2	712.6
$M_{18}{}^1\,M_{19}{}^1[3(+)]\cdots M_{10}{}^1[3(+)]$	789.2	760.4
$M_{10}{}^1[3(+)]\cdots M_{18}{}^1\,M_{19}{}^1[3(+)]$	807.6	743.2
$M_{12}{}^1\,M_{14}{}^1$	915.5	912.7
$M_8{}^1$	933.5	931.9
$M_9{}^1$	965.1	972.1
$M_8{}^1[3(+)]$	988.0	962.9
$M_9{}^1\,[3(+)]$	1019.9	…
$M_6{}^1$	∼1192[b]	1225.6[a]
$M_{18}{}^1\,M_{19}{}^1M_{29}{}^1\cdots M_{10}{}^1M_{29}{}^1$	1262.6	1257.2
$M_{10}{}^1M_{29}{}^1\cdots M_{18}{}^1\,M_{19}{}^1M_{29}{}^1$	1282.5	1240.0
M_8M_{29}	1462.8	1459[c]
M_9M_{29}	1494.4	…

[a]Part of a Fermi resonance – see Ref. 10.
[b]Present in a complicated FR, see text.
[c]Measured in ps-REMPI spectrum only, with a likely error of ±5 cm^{-1}.

IV. CONCLUSIONS

We have presented one-colour REMPI spectra in order to investigate the vibrations in the S_1 electronic state of Tol-h_8 and Tol-d_3 between 700 and 1500 cm^{-1}. The observed vibrations have been assigned based on quantum chemical calculations and ZEKE spectra recorded through a number of these features. Two Fermi resonances were observed in the S_1 electronic state of Tol-h_8; one at ∼750 cm^{-1} and a second at ∼1190 cm^{-1}. The zero-order states order states involved in the lower wavenumber Fermi resonance were unravelled for both isotopologues based on the vibrational activity observed in the ZEKE spectra recorded *via* each level. However, each ZEKE spectrum showed a broad "hump" in the baseline, an effect often concluded to be a result of significant IVR; such observations were primarily observed in the dispersed fluorescence spectra previously recorded *via* these levels.[3] The zero-order states involved in the higher wavenumber

TABLE VI. Experimentally derived fundamental vibrational wavenumbers (cm^{-1}) of the S_1 and cationic ground electronic states of Tol-h_8 and Tol-d_3.

	S_1		D_0^+	
M_i	$-h_8$	$-d_3$	$-h_8$	$-d_3$
		a_1		
6	~1190[a]		1232[a]	
8	934[a]	932[a]	980[a]	972[a]
9	966[a]	972[a]	990[a]	
10	755[a]	713[a]	767[b]	739[b]
11	457[b]	438[b]	496[b]	473[b]
		a_2		
14	226[b]	225[b]	335[b]	334[b]
		b_1		
18			566[a]	528[a]
19	314[b]	306[b]	377[b]	366[b]
20	145[b]	134[b]	151[b]	140[b]
		B_2		
29	532[b]	530[b]	477/486[b]	477[b]
30	331[b]	295[b]	342[b]	303[b]

[a]This work.
[b]Reference 1.

ranges were considerably more difficult to unravel; however, assignments of the vibrations which likely contribute to this Fermi resonance were made based on experimentally observed vibrations in both the S_1 and cation electronic states, in both this work and Ref. 1, and the results of time-resolved investigations both here and previously reported;[10] for Tol-h_8, the DF study by Hickman *et al.*[3] was also extremely useful. For the 1190 cm^{-1} FR in Tol-h_8, structure persisted in the ZEKE spectra recorded *via* two intermediate levels in Tol-h_8, but a broad "hump" in the baseline was again observed, while it was not possible to record a structured spectrum *via* a third intermediate level. This FR has been discussed here and in Ref. 10, with the involvement of the M_6 vibration and dissipative IVR being key. Furthermore, although many vibrations were observed in a similar wavenumber range of Tol-d_3, we were unable to record structured spectra *via* any of these levels. Some headway on the assignment was made, however, from the tr-SEVI spectra, which allowed a different ZOB to be identified. Intriguingly, ZEKE spectra recorded *via* intermediate levels lying between these two FR in Tol-h_8 showed no evidence for IVR, in support of conclusions made in a previous dispersed fluorescence study.[3] Overall, the results show that there is mode dependence of the IVR rates in these two isotopologues, and we have noted that it is critical not only for there to be a sufficient density of states for dissipative IVR to occur, but there must be a vibrational state available that facilitates coupling of the ZOB to this bath of states.

Subtle changes in wavenumbers of the vibrations of these two isotopologues result in dramatic changes in the vibrations observed in several wavenumber ranges, along with the coupling between them, notably so in the S_1 ~1190 cm^{-1} region. Knowledge of the fundamental vibrational wavenumbers, along with expectations of their changing wavenumber upon substitution, based upon the form of these vibrations,[2] not only allows the changing interactions between these vibrations to be unravelled, but may be used to predict when these vibrations are likely to fall into resonance.

Finally, in Tables V and VI, we present a summary of assigned bands in the REMPI and ZEKE spectra, respectively.

ACKNOWLEDGMENTS

We are grateful for funding from the Engineering and Physical Sciences Research Council (U.K.) EPSRC(GB) (Grant No. EP/E046150/1) and for studentships to A.M.Ga., A.M.Gr., and V.M.T.-R. We are grateful to Warren Lawrance and Jason Gascooke (Flinders University, Adelaide, Australia), for insightful discussion. Anna Andrejeva is thanked for her work in modifying the figures.

[1]A. M. Gardner, A. M. Green, V. M. Tamé-Reyes, V. H. K. Wilton, and T. G. Wright, J. Chem. Phys. **138**, 134303 (2013).
[2]A. M. Gardner and T. G. Wright, J. Chem. Phys. **135**, 114305 (2011).
[3]C. G. Hickman, J. R. Gascooke, and W. D. Lawrance, J. Chem. Phys. **104**, 4887 (1996).
[4]G. Herzberg, *Molecular Spectra and Molecular Structure II: Infrared and Raman Spectra of Polyatomic Molecules* (van Nostrand, New York, 1945).
[5]R. S. Mulliken, J. Chem. Phys. **23**, 1997 (1955).
[6]G. Varsányi, *Assignments of the Vibrational Spectra of Seven Hundred Benzene Derivatives* (John Wiley and Sons, New York, 1974), Vols. I and II.
[7]E. B. Wilson, Jr., Phys. Rev. **45**, 706 (1934).
[8]J. T. Meek, S. R. Long, and J. P. Reilly, J. Phys. Chem. **86**, 2809 (1982).
[9]P. T. Whiteside, A. K. King, J. A. Davies, K. L. Reid, M. Towrie, and P. Matousek, J. Chem. Phys. **123**, 204317 (2005).
[10]J. A. Davies, A. M. Green, A. M. Gardner, C. D. Withers, T. G. Wright, and K. L. Reid, Phys. Chem. Chem. Phys. **16**, 430 (2014).
[11]D. J. Nesbitt and R. W. Field, J. Phys. Chem. **100**, 12735 (1996).
[12]S. D. Gamblin, S. E. Daire, J. Lozeille, and T. G. Wright, Chem. Phys. Lett. **325**, 232 (2000).
[13]C. J. Hammond, V. L. Ayles, D. E. Bergeron, K. L. Reid, and T. G. Wright, J. Chem. Phys. **125**, 124308 (2006).
[14]A. R. Bacon and J. M. Hollas, Faraday Discuss. Chem. Soc. **86**, 129 (1988).
[15]V. L. Ayles, C. J. Hammond, D. E. Bergeron, O. J. Richards, and T. G. Wright, J. Chem. Phys. **126**, 244304 (2007).
[16]D. R. Borst and D. W. Pratt, J. Chem. Phys. **113**, 3658 (2000).
[17]K. T. Lu, G. C. Eiden, and J. C. Weisshaar, J. Phys. Chem. **96**, 9742 (1992).
[18]J. A. Davies, A. M. Green, and K. L. Reid, Phys. Chem. Chem. Phys. **12**, 9872 (2010).
[19]J. A. Davies and K. L. Reid, J. Chem. Phys. **135**, 124305 (2011).
[20]R. J. Doyle, E. S. J. Love, R. Da Campo, and S. R. Mackenzie, J. Chem. Phys. **122**, 194315 (2005).
[21]J. B. Hopkins, D. E. Powers, and R. E. Smalley, J. Chem. Phys. **72**, 5039 (1980).
[22]R. Vasudev and J. C. D. Brand, Chem. Phys. **37**, 211 (1979).
[23]J. R. Gascooke and W. D. Lawrance, J. Chem. Phys. **138**, 134302 (2013).
[24]P. Butler, D. B. Moss, H. Yin, T. W. Schmidt, and S. H. Kable, J. Chem. Phys. **127**, 094303 (2007).
[25]J. M. Blondeau and M. Stockburger, Ber. Bunsenges. Phys. Chem. **75**, 450 (1971).